



HAL
open science

From zero transmission to trapped modes in waveguides

Lucas Chesnel, Vincent Pagneux

► **To cite this version:**

Lucas Chesnel, Vincent Pagneux. From zero transmission to trapped modes in waveguides. 2018. hal-01952980v1

HAL Id: hal-01952980

<https://hal.science/hal-01952980v1>

Preprint submitted on 12 Dec 2018 (v1), last revised 2 Jan 2020 (v2)

HAL is a multi-disciplinary open access archive for the deposit and dissemination of scientific research documents, whether they are published or not. The documents may come from teaching and research institutions in France or abroad, or from public or private research centers.

L'archive ouverte pluridisciplinaire **HAL**, est destinée au dépôt et à la diffusion de documents scientifiques de niveau recherche, publiés ou non, émanant des établissements d'enseignement et de recherche français ou étrangers, des laboratoires publics ou privés.

From zero transmission to trapped modes in waveguides

LUCAS CHESNEL¹, VINCENT PAGNEUX²

¹ INRIA/Centre de mathématiques appliquées, École Polytechnique, Université Paris-Saclay, Route de Saclay, 91128 Palaiseau, France;

² Laboratoire d'Acoustique de l'Université du Maine, Av. Olivier Messiaen, 72085 Le Mans, France.

E-mails: `lucas.chesnel@inria.fr`, `vincent.pagneux@univ-lemans.fr`

– December 12, 2018–

Abstract. We consider the time-harmonic scattering wave problem in a 2D waveguide at wavenumber k such that one mode is propagating in the far field. In a first step, for a given k , playing with one scattering branch of finite length, we demonstrate how to construct geometries with zero transmission. The main novelty in this result is that the symmetry of the geometry is not needed : the proof relies on the unitary structure of the scattering matrix. Then, in a second step, from a waveguide with zero transmission, we show how to build geometries supporting trapped modes associated with eigenvalues embedded in the continuous spectrum. For this second construction, using the augmented scattering matrix and its unitarity, we play both with the geometry and the wavenumber. Finally, the mathematical analysis is supplemented by numerical illustrations of the results.

Key words. Waveguides, zero transmission, trapped modes, scattering matrix, asymptotic analysis.

1 Introduction

In this work, we are interested in the propagation of waves in a waveguide with two open channels (channels 1 and 2, see Figure 1). We work at a wavenumber k sufficiently small so that only one wave can propagate in each of the channels. For the Neumann problem that we consider in the following, which appears for example for acoustics, for water-waves or for electromagnetism, this wave is nothing but the planar wave. To describe the scattering process of the incident planar wave propagating in channel 1, classically one introduces two complex coefficients, namely the *reflection* and *transmission coefficients*, denoted s_{11} and s_{12} , such that s_{11} (resp. s_{12}) corresponds to the amplitude of the scattered field at infinity in channel 1 (resp. 2) (see (3)). According to the energy conservation, we have

$$|s_{11}|^2 + |s_{12}|^2 = 1.$$

In the first part of the article, we are interested in constructing non-symmetric geometries such that the transmission coefficient s_{12} is zero. In this case, all the energy is backscattered in channel 1, as if the waveguide was obstructed. This problem of *zero transmission* is interesting by itself and seems to have received little attention in literature, especially from a theoretical point of view. The motivation for designing domains where $s_{12} = 0$ is also linked to the second part of the paper where we show how to use them to find waveguides supporting so called *trapped modes* associated with eigenvalues embedded in the continuous spectrum. We remind the reader that trapped modes are non zero solutions of the homogeneous wave Problem (2) which are of finite energy. In particular, using Fourier decomposition, one shows that trapped modes are exponentially decaying at infinity. Unlike the zero transmission problem, the question of existence of trapped modes has been widely investigated in literature (see e.g. [46, 10, 11, 8, 22, 28, 37]). Note that eigenvalues embedded in

the continuous spectrum are also often called bound states in the continuum (BSCs or BICs) in quantum mechanics or in optics (see for example [41, 26, 16, 47, 15] as well as the recent review [19]).

One way to exhibit situations where $s_{12} = 0$ is to use the so-called Fano resonance (see the seminal paper [13] and the review article [25]). Let us present briefly the idea which is developed and justified in [44, 43, 45, 1, 5]. If trapped modes exist at a given wavenumber k_0 such that k_0^2 is an eigenvalue embedded in the continuous spectrum, then perturbing slightly the geometry allows one to exhibit settings where the scattering coefficients have a fast variation for k moving on the real axis around k_0 . And with an additional assumption of symmetry of the geometry, one can prove that $|s_{12}|$ passes exactly through 0 and 1. This process requires to start from a setting where it is known that there are trapped modes. We emphasize that trapped modes associated with eigenvalues embedded in the continuous spectrum are rather rare objects. In general, for a given geometry, the set of wavenumbers such that they exist is empty. Moreover, they are relatively unstable. If eigenvalues embedded in the continuous spectrum exist in a given setting, a small perturbation of the geometry will transform them into complex resonances as shown in [2] (except if the perturbation is carefully chosen, see [31]).

In the present article, in order to create geometries where $s_{12} = 0$, we follow another approach introduced in [6, 7]. As in [6, 7], we assume that the waveguide is endowed with a branch of finite length $L - 1$ (see Figure 1 left). The scattering coefficients depend on the geometry, in particular on L . Computing an asymptotic expansion of $s_{11} = s_{11}(L)$, $s_{12} = s_{12}(L)$ as $L \rightarrow +\infty$ allows us to know the main behaviour of the complex curves $L \mapsto s_{11}(L)$, $L \mapsto s_{12}(L)$. When the geometry has some symmetries, it is shown in [6, 7] that asymptotically $L \mapsto s_{11}(L)$, $L \mapsto s_{12}(L)$ pass through zero periodically. Then, owing to the symmetry assumption, we can get more and exhibit geometries where *zero reflection* ($s_{11} = 0$, $|s_{12}| = 1$), *zero transmission* ($|s_{11}| = 1$, $s_{12} = 0$) or *perfect invisibility* ($s_{11} = 0$, $s_{12} = 1$) occur (not only asymptotically but exactly). In the present work, quite surprisingly, we prove that without this assumption of symmetry of the geometry, asymptotically $L \mapsto s_{12}(L)$ still passes through zero periodically. And moreover, we show that the unitary structure of the scattering matrix defined in (4) is sufficient to conclude that $L \mapsto s_{12}(L)$ passes through zero exactly. We emphasize that without the assumption of symmetry, in general the curve for the reflection coefficient $L \mapsto s_{11}(L)$ does not pass through zero as $L \rightarrow +\infty$ (not even asymptotically). Thus, in the non-symmetric case we consider, we demonstrate zero transmission but zero reflection and so perfect invisibility, cannot be achieved.

In order to construct geometries supporting trapped modes, we will use a similar idea as before but with a useful auxiliary object called the augmented scattering matrix [33, 20, 27, 30] instead of the usual scattering matrix. To establish the existence of trapped modes, we will see that it is sufficient that a coefficient of the augmented scattering matrix, which is unitary, passes through the point of affix $-1 + 0i$. The unitary structure of the matrix will not be sufficient to obtain the desired result. But playing also a bit with the wavenumber, we will be able to circumvent the difficulty.

In the nicely written introduction of [17], from [16], the authors distinguish three main mechanisms to produce trapped modes associated with eigenvalues embedded in the continuous spectrum. The most common one is based on the decoupling between resonances and radiation modes due to symmetries of the problem [38, 39, 12, 11]. The second mechanism relies on the destructive interference between two resonances of a single resonator. It has been revealed by Friedrich and Wintgen in [14] (see also [41] and the review paper [35]). The third idea to obtain trapped modes consists in using two resonant structures acting as a pair of mirrors. Tuning correctly the distance between the two mirrors, one can trap waves between them, the structure then being equivalent to a Fabry-Perot cavity. This technique has been used in [24, 21, 40, 36, 4, 42]. The latter mechanism is the one we will exploit in the present article. On the other hand, we shall limit ourselves to Helmholtz equation with Neumann boundary conditions. Dirichlet boundary conditions (for quantum waveguides for example) can be treated completely similarly. Thus, we can construct quantum

waveguides supporting trapped modes.

All through the article, for the sake of simplicity, we shall restrict to a very simple 2D waveguide. However, the techniques can be extended in a straightforward way to higher dimension and more complex geometries (see the discussion in Section 5). We will consider scattering problems in T-shaped waveguides. In [29, 34], the authors study the existence of discrete spectrum (spectrum below the continuous spectrum) for Dirichlet problems in such geometries. Let us mention also that the present work shares connections with [41, 9, 3, 17]. In the latter papers, the authors investigate the existence of trapped modes associated with eigenvalues embedded in the continuous spectrum in geometries similar to ours via numerical investigations or simplified models.

The outline is as follows. In Section 2, for a given wavenumber below the first positive thresholds (monomode case), we explain how to construct geometries where the transmission coefficient is zero. In Section 3, we show how to design situations, playing both with the geometry and the wavenumber, such that trapped modes exist. In Section 4, we provide numerical illustrations of the results. In the conclusion, we discuss possible generalizations of the present approach as well as open questions. Finally, in a short Annex, we detail the proofs of two auxiliary results used in the analysis. The main results of this work are Theorem 2.1 (zero transmission) and Theorem 3.1 (existence of trapped modes).

2 Zero transmission

In this first section, for a given wavenumber we explain how to construct waveguides where the transmission coefficient is zero.

2.1 Setting

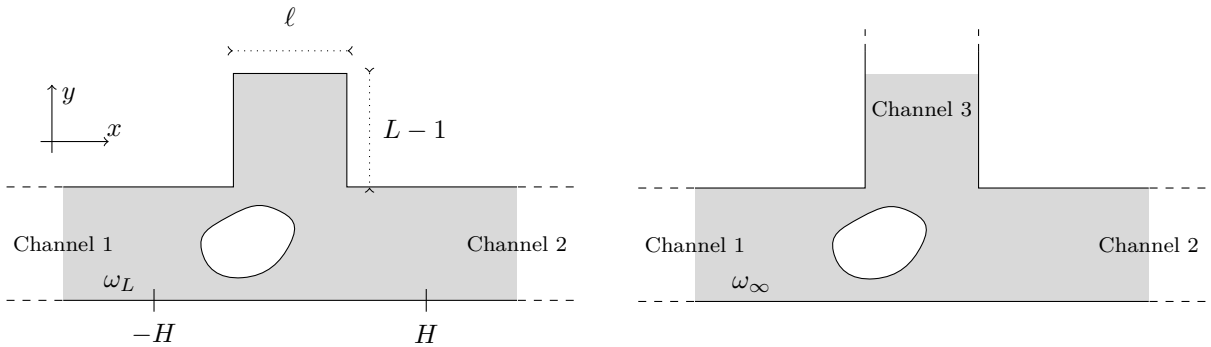


Figure 1: Geometries of ω_L (left) and ω_∞ (right).

For $\ell > 0$ and $L > 1$, let $\omega_L \subset \mathbb{R}^2$ be an open set which coincides with the domain

$$\{(x, y) \in \mathbb{R} \times (0; 1) \cup (-\ell/2; \ell/2) \times [1; L]\} \quad (1)$$

outside a bounded region independent of ℓ, L . We assume that ω_L is connected and has Lipschitz boundary $\partial\omega_L$. We call channel 1 (resp. channel 2) the branch of ω_L which coincides at infinity with $(-\infty; 0) \times (0; 1)$ (resp. with $(0; +\infty) \times (0; 1)$) (see Figure 1 left). We work in an academic geometry for the ease of presentation. In the conclusion (Section 5), we discuss possible extensions (see also Figure 7 right). We consider the problem with Neumann boundary condition

$$\begin{cases} \Delta u + k^2 u = 0 & \text{in } \omega_L \\ \partial_n u = 0 & \text{on } \partial\omega_L. \end{cases} \quad (2)$$

Here Δ is the 2D Laplace operator, k corresponds to the wavenumber. Moreover, n stands for the normal unit vector to $\partial\omega_L$ directed to the exterior of ω_L . We take $k \in (0; \pi)$ so that

$$w_1^\pm(x, y) = \frac{1}{\sqrt{2k}} e^{\mp ikx} \quad \text{and} \quad w_2^\pm(x, y) = \frac{1}{\sqrt{2k}} e^{\pm ikx}$$

are the only propagating modes in channels 1 and 2. More precisely, for $i = 1, 2$, the planar mode w_i^+ (resp. w_i^-) is outgoing (resp. ingoing) in channel i . Introduce $\chi_l \in \mathcal{C}^\infty(\mathbb{R}^2)$ (resp. $\chi_r \in \mathcal{C}^\infty(\mathbb{R}^2)$) a cut-off function equal to one for $x \leq -2H$ (resp. $x \geq 2H$) and to zero for $x \geq -H$ (resp. $x \leq H$). Here H is a parameter such that ω_L coincides with $\mathbb{R} \times (0; 1)$ for $|x| > H$. In order to describe the scattering process of the incident waves w_i^- propagating in channel i , we introduce the following scattering solutions

$$\begin{aligned} u_1 &= \chi_l (w_1^- + s_{11} w_1^+) + \chi_r s_{12} w_2^+ + \tilde{u}_1 \\ u_2 &= \chi_l s_{21} w_1^+ + \chi_r (w_2^- + s_{22} w_2^+) + \tilde{u}_2, \end{aligned} \tag{3}$$

where $s_{ij} \in \mathbb{C}$ and where \tilde{u}_1, \tilde{u}_2 decay exponentially as $O(e^{-\sqrt{\pi^2 - k^2}|x|})$ for $x \rightarrow \pm\infty$. It is known (see e.g. [32, Chap. 5, §3.3, Thm. 3.5 p.160]) that Problem (2) admits solutions of the form (3). The complex constants s_{ij} , $i, j \in \{1, 2\}$ in (3) are uniquely defined. Moreover the scattering matrix

$$\mathbb{S} := \begin{pmatrix} s_{11} & s_{12} \\ s_{21} & s_{22} \end{pmatrix} \in \mathbb{C}^{2 \times 2} \tag{4}$$

is unitary ($\mathbb{S}\overline{\mathbb{S}}^\top = \text{Id}^{2 \times 2}$) and we have $s_{21} = s_{12}$, i.e. \mathbb{S} is symmetric (even for a non symmetric geometry). For the proof of the two latter properties, see Lemma 6.1 in Annex. Classically, s_{11}, s_{22} are called *reflection coefficients* while $s_{12} = s_{21}$ are *transmission coefficients*. In this section, for a given wavenumber $k \in (0; \pi)$, we explain how to construct geometries such that $s_{12} = 0$.

2.2 Asymptotic analysis of the scattering coefficients

The scattering coefficients defined in (3), (4) depend on the geometry, in particular on L . In this paragraph, we compute an asymptotic expansion of $s_{11} = s_{11}(L)$, $s_{12} = s_{21}(L)$, $s_{22} = s_{22}(L)$ as $L \rightarrow +\infty$. In the analysis, the properties of Problem (2) set in the geometry ω_∞ (see (1) right) obtained from ω_L making $L \rightarrow +\infty$, play a key role. We call channel 3 the branch of ω_∞ which coincides at infinity with $(-\ell/2; \ell/2) \times (0; +\infty)$ (see Figure 1 right). Channels 1 and 2 of ω_∞ are defined as for ω_L . We assume that $\ell \in (0; \pi/k)$ so that

$$w_3^\pm(x, y) = \frac{1}{\sqrt{2k\ell}} e^{\pm iky}$$

are the only propagating modes in channel 3. For $\ell > \pi/k$, the analysis below must be adapted (see [6, Section 5] for more details). In ω_∞ , there are the solutions

$$\begin{aligned} u_1^\infty &= \chi_l (w_1^- + s_{11}^\infty w_1^+) + \chi_r s_{12}^\infty w_2^+ + \chi_t s_{13}^\infty w_3^+ + \tilde{u}_1^\infty \\ u_2^\infty &= \chi_l s_{21}^\infty w_1^+ + \chi_r (w_2^- + s_{22}^\infty w_2^+) + \chi_t s_{23}^\infty w_3^+ + \tilde{u}_2^\infty \\ u_3^\infty &= \chi_l s_{31}^\infty w_1^+ + \chi_r s_{32}^\infty w_2^+ + \chi_t (w_3^- + s_{33}^\infty w_3^+) + \tilde{u}_3^\infty, \end{aligned} \tag{5}$$

where $\tilde{u}_1^\infty, \tilde{u}_2^\infty, \tilde{u}_3^\infty$ decay exponentially at infinity. Here $\chi_t \in \mathcal{C}^\infty(\mathbb{R}^2)$ is a cut-off function equal to one for $y \geq 1 + 2\tau$ and to zero for $y \leq 1 + \tau$, where $\tau \geq 0$ is a given constant such that ω_∞ coincides with $(-\ell/2; \ell/2) \times \mathbb{R}$ for $y \geq \tau$. The scattering matrix

$$\mathbb{S}^\infty := \begin{pmatrix} s_{11}^\infty & s_{12}^\infty & s_{13}^\infty \\ s_{21}^\infty & s_{22}^\infty & s_{23}^\infty \\ s_{31}^\infty & s_{32}^\infty & s_{33}^\infty \end{pmatrix} \in \mathbb{C}^{3 \times 3} \tag{6}$$

is uniquely defined, unitary ($\mathbb{S}^\infty \overline{\mathbb{S}^\infty}^\top = \text{Id}^{3 \times 3}$) and symmetric (work as in the proof of Lemma 6.1 in Annex to show the two latter properties). For u_1, u_2 , following for example [23, Chap. 5, §5.6], we make the ansatz

$$\begin{aligned} u_1 &= u_1^\infty + a_1(L) u_3^\infty + \dots \\ u_2 &= u_2^\infty + a_2(L) u_3^\infty + \dots \end{aligned} \quad (7)$$

where $a_1(L), a_2(L)$ are some gauge functions to determine and where the dots correspond to small remainders. On $(-\ell/2; \ell/2) \times \{L\}$, the conditions $\partial_n u_1 = 0, \partial_n u_2 = 0$ lead to choose $a_1(L), a_2(L)$ such that

$$\begin{aligned} s_{13}^\infty e^{ikL} + a_1(L) (-e^{-ikL} + s_{33}^\infty e^{ikL}) = 0 &\Leftrightarrow a_1(L) = \frac{s_{13}^\infty}{e^{-2ikL} - s_{33}^\infty} \\ s_{23}^\infty e^{ikL} + a_2(L) (-e^{-ikL} + s_{33}^\infty e^{ikL}) = 0 &\Leftrightarrow a_2(L) = \frac{s_{23}^\infty}{e^{-2ikL} - s_{33}^\infty}. \end{aligned}$$

We shall consider ansatz (7) when $|s_{33}^\infty| \neq 1$ (when $|s_{33}^\infty| = 1$, see §6.2 in Annex). In this case, the gauge functions $a_1(L), a_2(L)$ are well-defined for all $L > 1$. Then we can prove that $\mathbb{S} = \mathbb{S}^{\text{asy}}(L) + \dots$, with

$$\mathbb{S}^{\text{asy}}(L) := (s_{ij}^{\text{asy}})_{1 \leq i, j \leq 2} = \begin{pmatrix} s_{11}^\infty & s_{12}^\infty \\ s_{21}^\infty & s_{22}^\infty \end{pmatrix} + \begin{pmatrix} a_1(L) \\ a_2(L) \end{pmatrix} \begin{pmatrix} s_{31}^\infty & s_{32}^\infty \end{pmatrix}. \quad (8)$$

In other words, we get

$$\begin{aligned} s_{11} &= s_{11}^\infty + \frac{s_{13}^\infty s_{31}^\infty}{e^{-2ikL} - s_{33}^\infty} + \dots & s_{12} &= s_{12}^\infty + \frac{s_{13}^\infty s_{32}^\infty}{e^{-2ikL} - s_{33}^\infty} + \dots \\ s_{21} &= s_{21}^\infty + \frac{s_{23}^\infty s_{31}^\infty}{e^{-2ikL} - s_{33}^\infty} + \dots & \text{and} & & s_{22} &= s_{22}^\infty + \frac{s_{23}^\infty s_{32}^\infty}{e^{-2ikL} - s_{33}^\infty} + \dots \end{aligned} \quad (9)$$

Here the dots stand for exponentially small terms. More precisely, we can establish (work as in [23, Chap. 5, §5.6], [6, Prop. 8.1]) an error estimate of the form $\|\mathbb{S} - \mathbb{S}^{\text{asy}}(L)\| \leq C e^{-\beta_\ell L}$ where C is a constant independent of $L > 1$ and $\beta_\ell := \sqrt{(\pi/\ell)^2 - k^2}$. Since \mathbb{S}^∞ is symmetric, we see from (9) that $\mathbb{S}^{\text{asy}}(L)$ is also symmetric. Moreover, after some calculations reproduced in the proof of Lemma 6.2 in Annex and based on the fact that \mathbb{S}^∞ is unitary, one can check that for all $L > 1$, the matrix $\mathbb{S}^{\text{asy}}(L)$ is unitary. Denote $\mathcal{C} := \{z \in \mathbb{C} \mid |z| = 1\}$ the unit circle. As L tends to $+\infty$, the coefficients $s_{11}^{\text{asy}}, s_{12}^{\text{asy}} = s_{21}^{\text{asy}}$ and s_{22}^{asy} run respectively on the sets

$$\gamma_{11} := \left\{ s_{11}^\infty + \frac{s_{13}^\infty s_{31}^\infty}{z - s_{33}^\infty} \mid z \in \mathcal{C} \right\}, \quad \gamma_{12} := \left\{ s_{12}^\infty + \frac{s_{13}^\infty s_{32}^\infty}{z - s_{33}^\infty} \mid z \in \mathcal{C} \right\}, \quad \gamma_{22} := \left\{ s_{22}^\infty + \frac{s_{23}^\infty s_{32}^\infty}{z - s_{33}^\infty} \mid z \in \mathcal{C} \right\}. \quad (10)$$

Using classical results concerning the Möbius transform (see e.g. [18, Chap. 5]), one finds that $\gamma_{11}, \gamma_{12}, \gamma_{22}$ are circles centered respectively at

$$z_{11} := s_{11}^\infty + \frac{s_{13}^\infty \overline{s_{33}^\infty} s_{31}^\infty}{1 - |s_{33}^\infty|^2}, \quad z_{12} := s_{12}^\infty + \frac{s_{13}^\infty \overline{s_{33}^\infty} s_{32}^\infty}{1 - |s_{33}^\infty|^2}, \quad z_{22} := s_{22}^\infty + \frac{s_{23}^\infty \overline{s_{33}^\infty} s_{32}^\infty}{1 - |s_{33}^\infty|^2} \quad (11)$$

of radii

$$\rho_{11} := \frac{|s_{13}^\infty s_{31}^\infty|}{1 - |s_{33}^\infty|^2}, \quad \rho_{12} := \frac{|s_{13}^\infty s_{32}^\infty|}{1 - |s_{33}^\infty|^2}, \quad \rho_{22} := \frac{|s_{23}^\infty s_{32}^\infty|}{1 - |s_{33}^\infty|^2}. \quad (12)$$

In the following, we assume that the coefficients $s_{12}^\infty, s_{13}^\infty, s_{23}^\infty$ in (5) are such that $s_{12}^\infty s_{13}^\infty s_{23}^\infty \neq 0$. This assumption is needed so that couplings exist between the three channels of ω_∞ . We refer the reader to §4.1 for an example of situation where numerically this assumption is satisfied. When $s_{12}^\infty s_{13}^\infty s_{23}^\infty \neq 0$, as a consequence of the unitary structure of \mathbb{S}^∞ , we have $|s_{33}^\infty| \neq 1$ and the three radii $\rho_{11}, \rho_{12}, \rho_{22}$ are located in $(0; 1)$.

Proposition 2.1. *Assume that the coefficients $s_{12}^\infty, s_{13}^\infty, s_{23}^\infty$ in (5) satisfy $s_{12}^\infty s_{13}^\infty s_{23}^\infty \neq 0$. Then the circle γ_{12} (the asymptotic orbit for the transmission coefficient) passes through zero.*

Proof. We have

$$s_{12}^\infty + \frac{s_{13}^\infty s_{32}^\infty}{z - s_{33}^\infty} = 0 \quad \Leftrightarrow \quad z = s_{33}^\infty - \frac{s_{13}^\infty s_{32}^\infty}{s_{12}^\infty}.$$

Therefore, it is sufficient to prove that

$$\left| s_{33}^\infty - \frac{s_{13}^\infty s_{32}^\infty}{s_{12}^\infty} \right| = 1. \quad (13)$$

Set $C = |s_{33}^\infty|^2 |s_{12}^\infty|^2 + |s_{13}^\infty|^2 |s_{32}^\infty|^2 - 2 \Re (s_{13}^\infty \overline{s_{33}^\infty} s_{32}^\infty \overline{s_{12}^\infty}) - |s_{12}^\infty|^2$. A direct computation shows that (13) is true if and only if $C = 0$. Since \mathbb{S}^∞ is unitary, we have

$$s_{11}^\infty \overline{s_{31}^\infty} + s_{12}^\infty \overline{s_{32}^\infty} + s_{13}^\infty \overline{s_{33}^\infty} = 0 \quad \Leftrightarrow \quad s_{12}^\infty \overline{s_{32}^\infty} + s_{13}^\infty \overline{s_{33}^\infty} = -s_{11}^\infty \overline{s_{31}^\infty}.$$

Squaring the second equality above, we deduce that

$$2 \Re (s_{13}^\infty \overline{s_{33}^\infty} s_{32}^\infty \overline{s_{12}^\infty}) = |s_{11}^\infty|^2 |s_{31}^\infty|^2 - |s_{12}^\infty|^2 |s_{32}^\infty|^2 - |s_{13}^\infty|^2 |s_{33}^\infty|^2.$$

Using again the fact that \mathbb{S}^∞ is unitary, we can write

$$\begin{aligned} C &= |s_{33}^\infty|^2 (|s_{12}^\infty|^2 + |s_{13}^\infty|^2) + |s_{32}^\infty|^2 (|s_{12}^\infty|^2 + |s_{13}^\infty|^2) - |s_{11}^\infty|^2 |s_{31}^\infty|^2 - |s_{12}^\infty|^2 \\ &= |s_{33}^\infty|^2 (1 - |s_{11}^\infty|^2) + |s_{32}^\infty|^2 (1 - |s_{11}^\infty|^2) - |s_{11}^\infty|^2 |s_{31}^\infty|^2 - |s_{12}^\infty|^2 \\ &= 1 - |s_{31}^\infty|^2 - |s_{11}^\infty|^2 - |s_{12}^\infty|^2 = 0. \end{aligned}$$

This gives the desired result. \square

Proposition 2.1 together with the error estimate $\|\mathbb{S} - \mathbb{S}^{\text{asy}}(L)\| \leq C e^{-\beta_\varepsilon L}$ show that the curve $L \mapsto s_{12}(L)$ for the transmission coefficient goes as close as we wish to zero as $L \rightarrow +\infty$. In the next paragraph, we prove that due to the unitary structure of \mathbb{S} , the curve $L \mapsto s_{12}(L)$ passes exactly through zero.

2.3 Zero transmission

Now we state and prove the main result of this section.

Theorem 2.1. *Assume that the coefficients $s_{12}^\infty, s_{13}^\infty, s_{23}^\infty$ in (5) satisfy $s_{12}^\infty s_{13}^\infty s_{23}^\infty \neq 0$. Then the complex curve $L \mapsto s_{12}(L)$ for the transmission coefficient passes through zero an infinite number of times as $L \rightarrow +\infty$.*

Remark 2.1. *In Section 4, §4.1 below, we provide an example of situation where numerically the assumption of Theorem 2.1 is satisfied.*

Proof. According to Proposition 2.1, we know that there is $L_\star > 0$ such that $s_{12}^{\text{asy}}(L_\star) = 0$. Since $L \mapsto s_{12}^{\text{asy}}(L)$ is π/k -periodic (see (8), (9)), we deduce that $s_{12}^{\text{asy}}(L_\star + n\pi/k) = 0$ for all $n \in \mathbb{N} := \{0, 1, \dots\}$. Define the interval

$$I_n := \left(L_\star + \frac{n\pi}{k} - \frac{1}{n+1}; L_\star + \frac{n\pi}{k} + \frac{1}{n+1} \right).$$

Since the circle γ_{12} passes through zero, there is $\eta \in (-\pi/2; \pi/2]$ such that γ_{12} is tangent to the line $\{\rho e^{i\eta} \in \mathbb{C}, \rho \in \mathbb{R}\}$. Define the quadrants

$$\begin{aligned} Q_1 &:= \{\rho e^{i\theta} \in \mathbb{C} \mid \rho > 0, \eta - \pi/4 < \theta < \eta + \pi/4\} \\ Q_2 &:= \{\rho e^{i\theta} \in \mathbb{C} \mid \rho < 0, \eta - \pi/4 < \theta < \eta + \pi/4\}, \end{aligned}$$

see Figure 2. On I_n , the curve $L \mapsto s_{12}^{\text{asy}}(L)$ meets both quadrants Q_1 and Q_2 . On the other hand, we have $|s_{12}(L) - s_{12}^{\text{asy}}(L)| \leq C e^{-\beta_\varepsilon L}$. As a consequence, there is $N \in \mathbb{N}$ such that for all $n \geq N$, the maps $L \mapsto s_{12}(L)$ intersects both Q_1 and Q_2 on I_n .

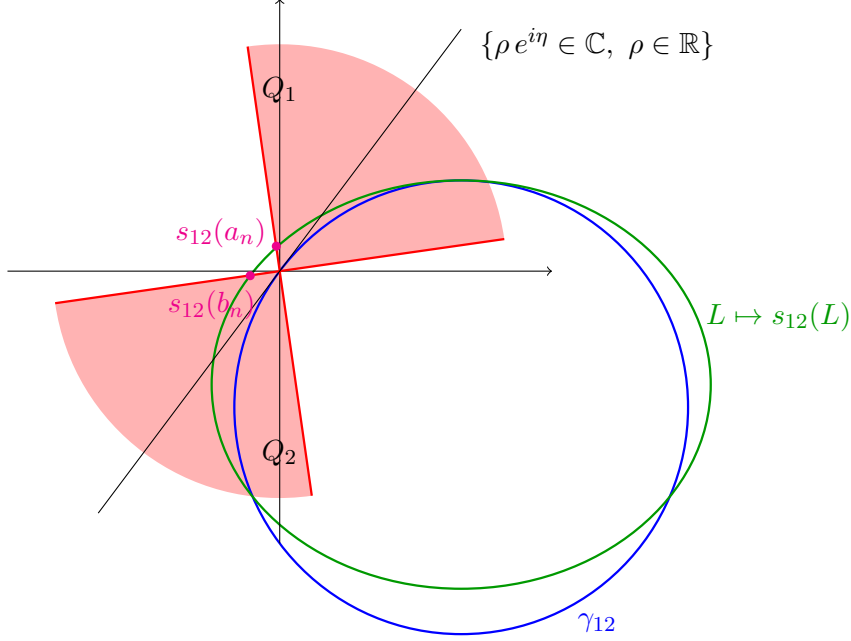


Figure 2: Notation used in the proof of Theorem 2.1.

Assume by contradiction that for all $n \geq N$, $L \mapsto s_{12}(L)$ does not pass through zero on I_n . Let us first describe the idea that we will use before making it rigorous. Since \mathbb{S} is unitary, there holds

$$s_{11}(L) \overline{s_{12}(L)} + s_{12}(L) \overline{s_{22}(L)} = 0. \quad (14)$$

As a consequence, we can write $s_{12}(L)/\overline{s_{12}(L)} = -s_{11}(L)/\overline{s_{22}(L)}$ for all $L \in I_n$. But if $L \mapsto s_{12}(L)$ does not pass through zero on I_n , the point $s_{12}(L)/\overline{s_{12}(L)} = e^{2i \arg(s_{12}(L))}$ must run rapidly on the unit circle for $L \in I_n$ as $n \rightarrow +\infty$. On the other hand, $s_{11}(L)/\overline{s_{22}(L)}$ tends to a constant on I_n as $n \rightarrow +\infty$. This way we obtain a contradiction. We emphasize that the unitary structure of \mathbb{S} is the key ingredient of the proof.

Now we make this discussion rigorous. If $L \mapsto s_{12}(L)$ does not vanish on I_n , since $L \mapsto s_{12}(L)$ is continuous and intersects both Q_1, Q_2 on I_n , we deduce that for all $n \geq N$, there are $a_n, b_n \in I_n$ such that $s_{12}(a_n) = t_n e^{i(\eta - \pi/4)}$ and $s_{12}(b_n) = \tilde{t}_n e^{i(\eta + \pi/4)}$, with $t_n, \tilde{t}_n \in \mathbb{R} \setminus \{0\}$. Taking successively $L = a_n, L = b_n$ in (14), we obtain

$$s_{11}(a_n) = -ie^{2i\eta} \overline{s_{22}(a_n)} \quad \text{and} \quad s_{11}(b_n) = ie^{2i\eta} \overline{s_{22}(b_n)}. \quad (15)$$

Pick ε small enough so that the open balls¹ $B(ie^{2i\eta} \overline{s_{22}^{\text{asy}}(L_\star)}, \varepsilon)$ and $B(-ie^{2i\eta} \overline{s_{22}^{\text{asy}}(L_\star)}, \varepsilon)$ do not intersect. This is possible because $|s_{22}^{\text{asy}}(L_\star)| = 1$ (remember that $s_{12}^{\text{asy}}(L_\star) = 0$). We know that there is M large enough such that, for all $n \geq M$, we have $s_{11}(a_n), s_{11}(b_n) \in B(s_{11}^{\text{asy}}(L_\star), \varepsilon/2)$ and $s_{22}(a_n), s_{22}(b_n) \in B(s_{22}^{\text{asy}}(L_\star), \varepsilon/2)$. From (15), we deduce that we must have both

$$B(s_{11}^{\text{asy}}(L_\star), \varepsilon/2) \cap B(ie^{2i\eta} \overline{s_{22}^{\text{asy}}(L_\star)}, \varepsilon/2) \neq \emptyset \quad \text{and} \quad B(s_{11}^{\text{asy}}(L_\star), \varepsilon/2) \cap B(-ie^{2i\eta} \overline{s_{22}^{\text{asy}}(L_\star)}, \varepsilon/2) \neq \emptyset.$$

This is impossible because there holds $B(\overline{s_{22}^{\text{asy}}(L_\star)}, \varepsilon) \cap B(-\overline{s_{22}^{\text{asy}}(L_\star)}, \varepsilon) = \emptyset$. This shows that for all $n \geq \max(M, N)$, $L \mapsto s_{12}(L)$ cancels on I_n . As a consequence, $L \mapsto s_{12}(L)$ passes through zero an infinite number of times as $L \rightarrow +\infty$. More precisely, it passes through zero almost periodically with a period π/k . \square

¹For $z_0 \in \mathbb{C}$ (resp. $z_0 \in \mathbb{R}^2$), $B(z_0, r)$ denotes the open ball of \mathbb{C} (resp. \mathbb{R}^2) of radius $r > 0$ centered at z_0 .

3 Trapped modes

In the previous section, for a given wavenumber $k_0 \in (0; \pi)$, we showed how to construct geometries with two open channels such that the transmission coefficient s_{12} defined in (3) is equal to zero. Now, from a given waveguide Ω_∞ where we know that $s_{12} = 0$, truncating one open channel, we explain how to find a geometry $\Omega_\mathcal{L}$ with one open channel supporting trapped modes for Problem (2) at wavenumbers k close to k_0 . We remind the reader that we say that u is a trapped mode for Problem (2) if u belongs to the Sobolev space $H^1(\Omega_\mathcal{L})$ and verifies (2). Note that Ω_∞ , the waveguide where $s_{12} = 0$, can result from the construction of the previous section ($\Omega_\infty = \omega_L$), but not necessarily.

3.1 Augmented scattering matrix

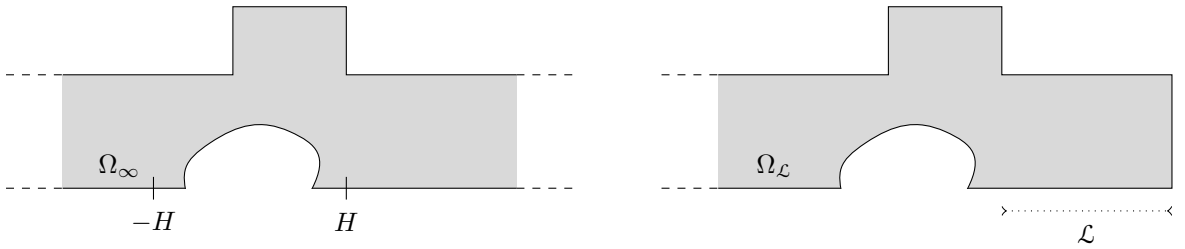


Figure 3: Geometries of Ω_∞ (left) and $\Omega_\mathcal{L}$ (right).

Let us start with a waveguide $\Omega_\infty \subset \mathbb{R}^2$ which coincides for $\pm x > H$, where $H > 0$ is given, with the strip $\mathbb{R} \times (0; 1)$ (see Figure 3 left). Again, this geometry is chosen only to simplify the presentation and other settings where the analysis below can be conducted are discussed in Section 5. For a given wavenumber $k \in (0; \pi)$, we assume that Ω_∞ is such that the transmission coefficient s_{12} appearing in (3) is equal to zero (zero transmission). We refer the reader to Section 2 or to [6, 7] for the construction of such domains. Then for $\mathcal{L} > 0$, we define the half-waveguide (unbounded in the left direction)

$$\Omega_\mathcal{L} := \{(x, y) \in \Omega_\infty \mid x < H + \mathcal{L}\}.$$

In the following, we explain how to find $\mathcal{L} > 0$ such that trapped modes exist for Problem (2) in $\Omega_\mathcal{L}$. We impose Neumann boundary conditions on $\{H + \mathcal{L}\} \times (0; 1)$ but we could also work with Dirichlet.

Set $\beta := \sqrt{\pi^2 - k^2}$ and

$$W_1^\pm(x, y) = w_1^\pm(x, y) = \frac{1}{\sqrt{2k}} e^{\mp ikx}, \quad W_2^\pm(x, y) = \frac{1}{\sqrt{2\beta}} (e^{-\beta x} \mp i e^{\beta x}) \cos(\pi y).$$

Note the particular definition of the functions W_2^\pm which are “wave packets”, combinations of exponentially decaying and growing modes as $x \rightarrow -\infty$. The normalisation coefficients for W_1^\pm , W_2^\pm are chosen so that the matrix defined in (17) is unitary. In [33, 20, 27, 30], it is proved that in the half-waveguide $\Omega_\mathcal{L}$, there are the solutions

$$\begin{aligned} U_1 &= W_1^- + S_{11} W_1^+ + S_{12} W_2^+ + \tilde{U}_1 \\ U_2 &= W_2^- + S_{21} W_1^+ + S_{22} W_2^+ + \tilde{U}_2 \end{aligned} \tag{16}$$

where \tilde{U}_1, \tilde{U}_2 decay as $O(e^{\sqrt{4\pi^2 - k^2}x})$ when $x \rightarrow -\infty$. The complex constants S_{ij} , $i, j \in \{1, 2\}$ in (16) are uniquely defined. They allow us to define the augmented scattering matrix introduced in [33, 20, 27, 30]

$$\mathfrak{S} := \begin{pmatrix} S_{11} & S_{12} \\ S_{21} & S_{22} \end{pmatrix} \in \mathbb{C}^{2 \times 2}. \tag{17}$$

Working exactly as in the proof of Lemma 6.1 in Annex, one can show that \mathcal{S} is unitary ($\mathcal{S}\bar{\mathcal{S}}^\top = \text{Id}^{2 \times 2}$) and symmetric ($S_{21} = S_{12}$). This augmented scattering matrix provides an algebraic criterion to detect the presence of trapped modes (see e.g. [30, Thm. 2]):

Lemma 3.1. *If $S_{22} = -1$, then U_2 is a trapped mode for Problem (2) set in $\Omega_{\mathcal{L}}$.*

Remark 3.1. *Note that $S_{22} = -1$ is only a sufficient criterion of existence of trapped modes. Indeed the geometry $\Omega_{\mathcal{L}}$ can support trapped modes for Problem (2) with $S_{22} \neq -1$. In this case, these trapped modes must decay as $O(e^{\sqrt{4\pi^2 - k^2}x})$ when $x \rightarrow -\infty$.*

Proof. If $S_{22} = -1$, since \mathcal{S} is unitary, then $S_{21} = 0$. In such a situation, according to (16), we have $U_2 = -i\sqrt{2/\beta}e^{\beta x}\cos(\pi y) + O(e^{\sqrt{4\pi^2 - k^2}x})$ as $x \rightarrow -\infty$. This shows that $U_2 \not\equiv 0$ belongs to $H^1(\Omega_{\mathcal{L}})$. In other words U_2 is a trapped mode. \square

3.2 Asymptotic analysis of the coefficients of the augmented scattering matrix

The augmented scattering matrix \mathcal{S} depends on \mathcal{L} . In this section, we compute an asymptotic expansion of all the elements of $\mathcal{S}(\mathcal{L})$ as $\mathcal{L} \rightarrow +\infty$. In particular, we will show that the dominant asymptotic term of $\mathcal{L} \mapsto S_{22}(\mathcal{L})$ hits the unit circle.

To proceed, we work exactly as in §2.2. In the geometry Ω_∞ (see Figure 3 right) obtained from $\Omega_{\mathcal{L}}$ making $\mathcal{L} \rightarrow +\infty$, there are the solutions

$$\begin{aligned} U_1^\infty &= \chi_l(W_1^- + S_{11}^\infty W_1^+ + S_{12}^\infty W_2^+) + \chi_r S_{13}^\infty W_1^+ + \tilde{U}_1^\infty \\ U_2^\infty &= \chi_l(W_2^- + S_{21}^\infty W_1^+ + S_{22}^\infty W_2^+) + \chi_r S_{23}^\infty W_1^+ + \tilde{U}_2^\infty \\ U_3^\infty &= \chi_l(S_{31}^\infty W_1^+ + S_{32}^\infty W_2^+) + \chi_r(W_1^- + S_{33}^\infty W_1^+) + \tilde{U}_3^\infty, \end{aligned}$$

where $\tilde{U}_1^\infty, \tilde{U}_2^\infty, \tilde{U}_3^\infty$ decay as $O(e^{\sqrt{4\pi^2 - k^2}x})$ for $x \rightarrow -\infty$ and as $O(e^{-\sqrt{\pi^2 - k^2}x})$ for $x \rightarrow +\infty$. Here χ_l, χ_r are the cut-off functions introduced in (3). The scattering matrix

$$\mathcal{S}^\infty := \begin{pmatrix} S_{11}^\infty & S_{12}^\infty & S_{13}^\infty \\ S_{21}^\infty & S_{22}^\infty & S_{23}^\infty \\ S_{31}^\infty & S_{32}^\infty & S_{33}^\infty \end{pmatrix} \in \mathbb{C}^{3 \times 3} \quad (18)$$

is unitary and symmetric. For U_1, U_2 , we make the ansatz

$$\begin{aligned} U_1 &= U_1^\infty + A_1(\mathcal{L})U_3^\infty + \dots \\ U_2 &= U_2^\infty + A_2(\mathcal{L})U_3^\infty + \dots \end{aligned}$$

On $\{H + L\} \times (0; 1)$, the conditions $\partial_n U_1 = 0, \partial_n U_2 = 0$ lead to choose $A_1(\mathcal{L}), A_2(\mathcal{L})$ such that

$$\begin{aligned} S_{13}^\infty e^{ik\mathcal{L}} + A_1(\mathcal{L})(-e^{-ik\mathcal{L}} + S_{33}^\infty e^{ik\mathcal{L}}) = 0 &\Leftrightarrow A_1(\mathcal{L}) = \frac{S_{13}^\infty}{e^{-2ik\mathcal{L}} - S_{33}^\infty} \\ S_{23}^\infty e^{ik\mathcal{L}} + A_2(\mathcal{L})(-e^{-ik\mathcal{L}} + S_{33}^\infty e^{ik\mathcal{L}}) = 0 &\Leftrightarrow A_2(\mathcal{L}) = \frac{S_{23}^\infty}{e^{-2ik\mathcal{L}} - S_{33}^\infty}. \end{aligned}$$

As in §2.2, we assume that $|S_{33}^\infty| \neq 1$ (see §6.2 in the Annex for the case $|S_{33}^\infty| = 1$). Then we have $\mathcal{S} = \mathcal{S}^{\text{asy}}(\mathcal{L}) + \dots$, with

$$\mathcal{S}^{\text{asy}}(\mathcal{L}) = (\mathcal{S}_{ij}^{\text{asy}})_{1 \leq i, j \leq 2} := \begin{pmatrix} S_{11}^\infty & S_{12}^\infty \\ S_{21}^\infty & S_{22}^\infty \end{pmatrix} + \begin{pmatrix} A_1(\mathcal{L}) \\ A_2(\mathcal{L}) \end{pmatrix} \begin{pmatrix} S_{31}^\infty & S_{32}^\infty \end{pmatrix}.$$

In other words, we have

$$\begin{aligned} S_{11} &= S_{11}^\infty + \frac{S_{13}^\infty S_{31}^\infty}{e^{-2ik\mathcal{L}} - S_{33}^\infty} + \dots & S_{12} &= S_{12}^\infty + \frac{S_{13}^\infty S_{32}^\infty}{e^{-2ik\mathcal{L}} - S_{33}^\infty} + \dots \\ S_{21} &= S_{21}^\infty + \frac{S_{23}^\infty S_{31}^\infty}{e^{-2ik\mathcal{L}} - S_{33}^\infty} + \dots & \text{and} & & S_{22} &= S_{22}^\infty + \frac{S_{23}^\infty S_{32}^\infty}{e^{-2ik\mathcal{L}} - S_{33}^\infty} + \dots \end{aligned} \quad (19)$$

The dots stand for exponentially small terms. More precisely, we can establish an error estimate of the form $\|\mathcal{S} - \mathcal{S}^{\text{asy}}(\mathcal{L})\| \leq C e^{-\beta\mathcal{L}}$ where C is a constant independent of $\mathcal{L} > 0$. Since \mathcal{S}^∞ is symmetric, $\mathcal{S}^{\text{asy}}(\mathcal{L})$ is also symmetric. Moreover working as in Lemma 6.2 in Annex, one can check that for all $\mathcal{L} > 0$, $\mathcal{S}^{\text{asy}}(\mathcal{L})$ is unitary. As \mathcal{L} tends to $+\infty$, the coefficients S_{11} , $S_{12} = S_{21}$ and S_{22} run respectively on the sets

$$\Gamma_{11} := \left\{ S_{11}^\infty + \frac{S_{13}^\infty S_{31}^\infty}{z - S_{33}^\infty} \mid z \in \mathcal{C} \right\}, \quad \Gamma_{12} := \left\{ S_{12}^\infty + \frac{S_{13}^\infty S_{32}^\infty}{z - S_{33}^\infty} \mid z \in \mathcal{C} \right\}, \quad \Gamma_{22} := \left\{ S_{22}^\infty + \frac{S_{23}^\infty S_{32}^\infty}{z - S_{33}^\infty} \mid z \in \mathcal{C} \right\}. \quad (20)$$

As in the previous section, one finds that Γ_{11} , Γ_{12} , Γ_{22} coincide with circles centered respectively at

$$Z_{11} := S_{11}^\infty + \frac{S_{13}^\infty \overline{S_{33}^\infty} S_{31}^\infty}{1 - |S_{33}^\infty|^2}, \quad Z_{12} := S_{12}^\infty + \frac{S_{13}^\infty \overline{S_{33}^\infty} S_{32}^\infty}{1 - |S_{33}^\infty|^2}, \quad Z_{22} := S_{22}^\infty + \frac{S_{23}^\infty \overline{S_{33}^\infty} S_{32}^\infty}{1 - |S_{33}^\infty|^2} \quad (21)$$

of radii

$$P_{11} := \frac{|S_{13}^\infty S_{31}^\infty|}{1 - |S_{33}^\infty|^2}, \quad P_{12} := \frac{|S_{13}^\infty S_{32}^\infty|}{1 - |S_{33}^\infty|^2}, \quad P_{22} := \frac{|S_{23}^\infty S_{32}^\infty|}{1 - |S_{33}^\infty|^2}. \quad (22)$$

Working exactly as in the proof of Proposition 2.1, we can show the following statement.

Proposition 3.1. *Assume that the coefficients S_{12}^∞ , S_{13}^∞ , S_{23}^∞ in (18) satisfy $S_{12}^\infty S_{13}^\infty S_{23}^\infty \neq 0$. Then the circle Γ_{12} passes through zero. As a consequence, since $\mathcal{S}^{\text{asy}}(\mathcal{L})$ is unitary, we deduce that the circles Γ_{11} , Γ_{22} intersect the unit circle \mathcal{C} at exactly one point.*

Remark 3.2. *From this proposition, it follows that the dominant asymptotic term of $\mathcal{L} \mapsto S_{22}(\mathcal{L})$ hits the unit circle. This is the property that will be used below to prove the existence of trapped modes.*

Remark 3.3. *As in the previous section, we assume that $S_{12}^\infty S_{13}^\infty S_{23}^\infty \neq 0$, which implies $|S_{33}^\infty| \neq 1$, so that couplings exist between the modes in Ω_∞ .*

3.3 The particular case where zero transmission occurs in Ω_∞

In Ω_∞ , there are also the classical solutions u_1 , u_2 introduced in (3) which allow one to define the usual scattering matrix $\mathbb{S} \in \mathbb{C}^{2 \times 2}$ in (4) (for the identity relating $\mathbb{S} \in \mathbb{C}^{2 \times 2}$ and $\mathcal{S}^\infty \in \mathbb{C}^{3 \times 3}$, we refer the reader to [30, Thm. 3]). In this section, we are interested in situations (geometries) where $s_{12} = s_{21} = 0$ (zero transmission). In this case, we establish an additional property for the asymptotic circle Γ_{22} defined in (20).

Proposition 3.2. *Assume that the coefficients S_{12}^∞ , S_{13}^∞ , S_{23}^∞ in (18) satisfy $S_{12}^\infty S_{13}^\infty S_{23}^\infty \neq 0$. Assume also that we have $s_{12} = 0$ (zero transmission in Ω_∞). Then the circle Γ_{22} intersects the unit circle \mathcal{C} at the point of affix $-1 + 0i$ (see Figure 9).*

Proof. If $s_{12} = 0$, starting from (3), we see that there is some $\lambda \in \mathbb{C}$ such that u_1 (defined in (3)) admits the expansion

$$u_1 = \chi_l (W_1^+ + s_{11} W_1^- + \lambda (W_2^+ - W_2^-)) + \hat{u}_1$$

with \hat{u}_1 which decays as $O(e^{\sqrt{4\pi^2 - k^2}x})$ for $x \rightarrow -\infty$ and as $O(e^{-\sqrt{\pi^2 - k^2}x})$ for $x \rightarrow +\infty$. Define the symplectic (sesquilinear and anti-hermitian ($q(u, v) = -\overline{q(v, u)}$)) form $q(\cdot, \cdot)$ such that for all $u, v \in H_{\text{loc}}^1(\Omega_\infty)$

$$q(u, v) = \int_{\Sigma_{-2H} \cup \Sigma_{2H}} \frac{\partial u}{\partial n} \bar{v} - u \frac{\partial \bar{v}}{\partial n} d\sigma. \quad (23)$$

Here $\Sigma_{\pm 2H} := \{\pm 2H\} \times (0; 1)$, $\partial_n = \pm \partial_x$ at $x = \pm 2H$ and $H_{\text{loc}}^1(\Omega_\infty)$ refers to the Sobolev space of functions φ such that $\varphi|_\Theta \in H^1(\Theta)$ for all bounded domains $\Theta \subset \Omega_\infty$. Using that U_2^∞ , U_3^∞ and u_1 satisfy the homogeneous Helmholtz equation in Ω_∞ , integrating by parts, one obtains $q(U_2^\infty, u_1) =$

$q(U_3^\infty, u_1) = 0$. On the other hand, decomposing these three functions in Fourier series on $\Sigma_{\pm 2H}$, one finds

$$0 = q(U_2^\infty, u_1) = S_{21}^\infty \overline{s_{11}} - S_{22}^\infty \overline{\lambda} - \overline{\lambda} \quad (24)$$

$$0 = q(U_3^\infty, u_1) = S_{31}^\infty \overline{s_{11}} - S_{32}^\infty \overline{\lambda}. \quad (25)$$

Coupling (24) and (25), we get the additional relation

$$S_{31}^\infty = \frac{S_{32}^\infty S_{21}^\infty}{1 + S_{22}^\infty} \quad (26)$$

for the coefficients of the augmented scattering matrix \mathcal{S}^∞ when $s_{12} = 0$. Note that since by assumption $S_{23}^\infty \neq 0$, we have $S_{22}^\infty \neq -1$. Actually the latter property is true as soon as there is no trapped mode in the geometry Ω_∞ . Now, we explain how to use Identity (26) to show that the circle Γ_{22} defined in (20) passes through the point of affix $-1 + 0i$. From (21), we know that the center of Γ_{22} is given by

$$Z_{22} = S_{22}^\infty + \frac{S_{23}^\infty \overline{S_{33}^\infty} S_{32}^\infty}{1 - |S_{33}^\infty|^2} = \frac{S_{22}^\infty (|S_{31}^\infty|^2 + |S_{32}^\infty|^2) + S_{23}^\infty \overline{S_{33}^\infty} S_{32}^\infty}{|S_{31}^\infty|^2 + |S_{32}^\infty|^2}.$$

Using that $S_{21}^\infty \overline{S_{31}^\infty} + S_{22}^\infty \overline{S_{32}^\infty} + S_{23}^\infty \overline{S_{33}^\infty} = 0$ (\mathcal{S}^∞ is unitary), we obtain

$$Z_{22} = \frac{S_{22}^\infty |S_{31}^\infty|^2 - S_{32}^\infty S_{21}^\infty \overline{S_{31}^\infty}}{|S_{31}^\infty|^2 + |S_{32}^\infty|^2}.$$

With (26), we deduce

$$\begin{aligned} Z_{22} &= \frac{|S_{32}^\infty|^2 |S_{21}^\infty|^2}{|S_{31}^\infty|^2 + |S_{32}^\infty|^2} \left(\frac{S_{22}^\infty}{|1 + S_{22}^\infty|^2} - \frac{1}{1 + \overline{S_{22}^\infty}} \right) = - \frac{|S_{32}^\infty|^2 |S_{21}^\infty|^2}{|S_{31}^\infty|^2 + |S_{32}^\infty|^2} \frac{1}{|1 + S_{22}^\infty|^2} \\ &= - \frac{|S_{31}^\infty|^2}{|S_{31}^\infty|^2 + |S_{32}^\infty|^2} = -1 + P_{22}. \end{aligned}$$

The last equality in the above equation has been obtained using the expression of P_{22} in (22). Since P_{22} stands for the radius of Γ_{22} , this shows that Γ_{22} passes through the point of affix $-1 + 0i$. \square

Proposition 3.2 together with the error estimate $\|\mathcal{S} - \mathcal{S}^{\text{asy}}(\mathcal{L})\| \leq C e^{-\beta \mathcal{L}}$ show that the curve $\mathcal{L} \mapsto S_{22}(\mathcal{L})$ passes as close as we wish to the point of affix $-1 + 0i$ as $\mathcal{L} \rightarrow +\infty$ when we know that $s_{12} = 0$. Unfortunately, contrary to what has been done in the previous section to prove that $L \mapsto s_{12}(L)$ passes through zero as $L \rightarrow +\infty$ (see the proof of Theorem 2.1), the unitary structure of \mathcal{S} is not sufficient to guarantee that $\mathcal{L} \mapsto S_{22}(\mathcal{L})$ passes exactly through the point of affix $-1 + 0i$ as $\mathcal{L} \rightarrow +\infty$. In our analysis, we will have to play also with the wavenumber k .

Remark 3.4. *Let us present a simple calculation allowing one to feel that the situation $s_{12} = 0$ in Ω_∞ is interesting to construct trapped modes in $\Omega_{\mathcal{L}}$. When $s_{12} = s_{21} = 0$, the function u_2 in (3) admits the expansion*

$$u_2 = \chi_r (w_2^- + s_{22} w_2^+) + \tilde{u}_2,$$

where \tilde{u}_2 decays exponentially as $x \rightarrow \pm\infty$. Due to conservation of energy, $s_{12} = 0$ implies $s_{22} = e^{i\eta}$ for some $\eta \in [0; 2\pi)$. As a consequence, on $\{H + \mathcal{L}\} \times (0; 1)$, we find $\partial_n(w_2^- + s_{22} w_2^+) = ik(-e^{-ik(H+\mathcal{L})} + e^{i\eta} e^{ik(H+\mathcal{L})})/\sqrt{2k}$. Thus, there is a periodic sequence (\mathcal{L}_n) such that $\partial_n(w_2^- + s_{22} w_2^+) = 0$ on $\{\mathcal{L}_n\} \times (0; 1)$. Of course, this does not show that u_2 is a trapped mode in $\Omega_{\mathcal{L}_n}$ ($\partial_n u_2$ is exponentially small on $\{H + \mathcal{L}_n\} \times (0; 1)$ but not zero). However it leads to think there is a trapped mode ‘‘close to’’ $(k, \Omega_{\mathcal{L}_n})$.

3.4 Proof of existence of trapped modes

The coefficient S_{22} depends both on \mathcal{L} and k . Up to now, we have found pairs (\mathcal{L}, k) such that the dominant asymptotic term of S_{22} is equal to -1 . Now, we will show that there is a sequence (\mathcal{L}_n, k_n) such that we have exactly $S_{22} = -1$ (indeed, from Lemma 3.1, we know that this proves the existence of trapped modes).

Assume that there is $k_0 \in (0; \pi)$ such that the transmission coefficient s_{12} in (3) is zero. Assume also that the coefficients $S_{12}^\infty, S_{13}^\infty, S_{23}^\infty$ in (18) satisfy $S_{12}^\infty S_{13}^\infty S_{23}^\infty \neq 0$ at the wavenumber k_0 . Since \mathcal{S}^∞ depend smoothly on the wavenumber, there is $\varepsilon > 0$ such that we have $S_{12}^\infty S_{13}^\infty S_{23}^\infty \neq 0$ for all $k \in [k_0 - \varepsilon; k_0 + \varepsilon]$. For $k \in [k_0 - \varepsilon; k_0 + \varepsilon]$, as $\mathcal{L} \rightarrow +\infty$, we know from Proposition 3.1 that there is a sequence $(\mathcal{L}_n(k))$ such that $|S_{22}(\mathcal{L}_n(k), k)| = 1$. Introduce $\alpha_n(k) \in [0; 2\pi)$ such that

$$S_{22}(\mathcal{L}_n(k), k) = e^{i\alpha_n(k)}.$$

The sequence $(\alpha_n(k))$ tends to $\alpha_\infty(k)$ where $\alpha_\infty(k) \in [0; 2\pi)$ is such that

$$\Gamma_{22}(k) \cap \mathcal{C} = \{e^{i\alpha_\infty(k)}\}.$$

Assume that

$$\text{The map } k \mapsto \Im m Z_{22}(k) \text{ changes sign at } k = k_0. \quad (27)$$

We remind the reader that Z_{22} is the center of the circle Γ_{22} defined in (21) such that $\Im m Z_{22}(k_0) = 0$ (Proposition 3.2). Observe that (27) is true for example if $\Im m \partial_k Z_{22}|_{k=k_0} \neq 0$. In this case, since $\alpha_\infty(k_0) = \pi$ (again Proposition 3.2), we know that there is $\varepsilon > 0$ (smaller than the already introduced $\varepsilon > 0$) such that $\alpha_\infty(k_0 - \varepsilon) - \pi$ and $\alpha_\infty(k_0 + \varepsilon) - \pi$ have different signs. Pick $N \in \mathbb{N}$ large enough so that for all $n \geq N$, the quantities $\alpha_n(k_0 - \varepsilon) - \pi$ and $\alpha_n(k_0 + \varepsilon) - \pi$ have different signs. Since the map $k \mapsto \alpha_n(k)$ is continuous, we know that there is $k_n^* \in [k_0 - \varepsilon; k_0 + \varepsilon]$ such that $\alpha_n(k_n^*) = \pi$. Then we have

$$S_{22}(\mathcal{L}_n(k_n^*), k_n^*) = e^{i\alpha_n(k_n^*)} = -1.$$

This shows the existence of trapped modes for Problem (2) at the wavenumber k_n^* in the geometry $\Omega_{\mathcal{L}_n(k_n^*)}$. Note that as $n \rightarrow +\infty$, we have $k_n^* \rightarrow k_0$. Moreover, $(\mathcal{L}_n(k_n^*))$ is almost periodic of period π/k . We summarize these results in the following theorem.

Theorem 3.1. *Assume that there holds $s_{12} = 0$ (zero transmission in Ω_∞) at the wavenumber $k_0 \in (0; \pi)$. Assume also that the coefficients $S_{12}^\infty, S_{13}^\infty, S_{23}^\infty$ in (18) satisfy $S_{12}^\infty S_{13}^\infty S_{23}^\infty \neq 0$ at the wavenumber k_0 and that (27) is true. Then there are sequences $(\mathcal{L}_n), (k_n)$ such that Problem (2) admits trapped modes in the geometry $\Omega_{\mathcal{L}_n}$ at the wavenumber k_n . Moreover, there hold $\lim_{n \rightarrow +\infty} \mathcal{L}_n = +\infty$ and $\lim_{n \rightarrow +\infty} k_n = k_0$.*

Remark 3.5. *In Section 4, §4.2 below, we provide an example of situation where numerically the assumptions of Theorem 3.1 are satisfied.*

4 Numerical experiments

4.1 Zero transmission

In the first series of experiments, we set $M := (0.2, 0.4)$ and

$$\omega_L := \{(x, y) \in \mathbb{R} \times (0; 1) \cup (-1/2; 1/2) \times [1; L)\} \setminus \overline{B(M, 0.3)}$$

(see Figure 6). Here $B(M, 0.3)$ corresponds to the open ball centered at M of radius 0.3. Note that there is no symmetry in the geometry. For each L in a given range, we compute numerically the coefficients of the scattering matrix $\mathbb{S} \in \mathbb{C}^{2 \times 2}$ defined in (4). To proceed, we use a P2 finite element method in a truncated waveguide. On the artificial boundary created by the truncation, a Dirichlet-to-Neumann operator with 15 terms serves as a transparent condition. We take $k = 0.8\pi$

and $\ell = 1$. In Figure 4, we display the scattering coefficients for $L \in (1.1; 6)$. In accordance with the results obtained in §2.2, we observe that when $L \rightarrow +\infty$, asymptotically $L \mapsto s_{11}(L)$, $L \mapsto s_{12}(L)$ and $L \mapsto s_{22}(L)$ run on circles. More precisely, computing the coefficients of the scattering matrix $\mathbb{S}^\infty \in \mathbb{C}^{3 \times 3}$ defined in (6), we indeed check that asymptotically $L \mapsto s_{11}(L)$, $L \mapsto s_{12}(L)$ and $L \mapsto s_{22}(L)$ run respectively on the circles γ_{11} , γ_{12} and γ_{22} obtained in (20). The asymptotic sets γ_{11} , γ_{12} , γ_{22} are displayed in Figure 4 but are mostly covered by the marks of $s_{11}(L)$, $s_{12}(L)$, $s_{22}(L)$ (we remind the reader that the convergence is exponentially fast). We also note that, as predicted by Theorem 2.1, the curve $L \mapsto s_{12}(L)$ indeed passes through zero as $L \rightarrow +\infty$.

In Figure 5, we display the curve $L \mapsto -\ln |s_{12}(L)|$ for $L \in (1.1; 6)$. The peaks correspond to the values of L such that $s_{12}(L) = 0$ (zero transmission). According to the proof of Theorem 2.1, we expect that the peaks are almost periodic with a distance between two peaks tending to $\pi/k = 1.25$ as $L \rightarrow +\infty$. The numerical results we get are coherent with this value. Finally, in Figure 6, we represent the real part of the total field u_1 defined in (3) for $L = 2.496$ (second peak of Figure 5). We can observe that the field is indeed exponentially decaying as $x \rightarrow +\infty$.

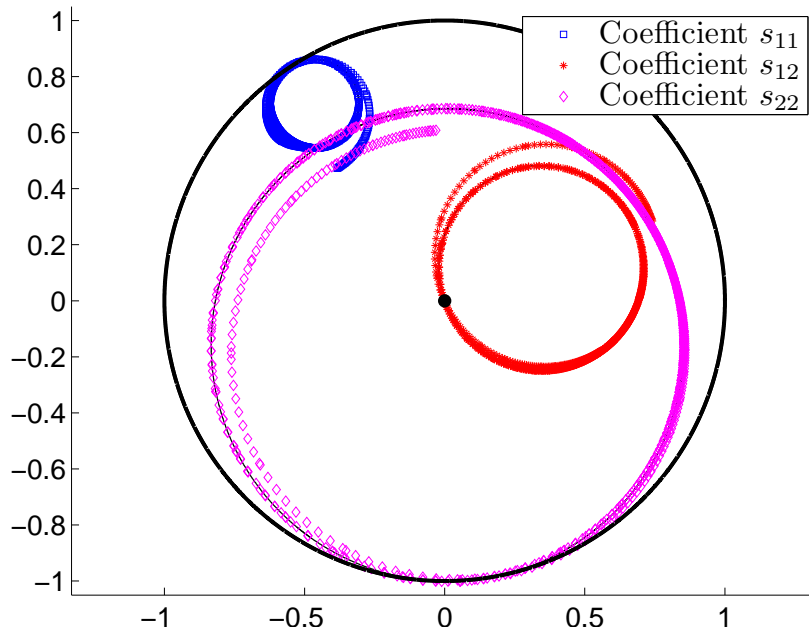


Figure 4: Coefficients $L \mapsto s_{11}(L)$, $L \mapsto s_{12}(L)$ and $L \mapsto s_{22}(L)$ for $L \in (1.1; 6)$. The thin black circles (mostly hidden by the symbols) correspond to the asymptotic circles γ_{11} , γ_{12} and γ_{22} defined in (20). According to the conservation of energy, we know that the scattering coefficients are located inside the unit disk marked by the black bold line.

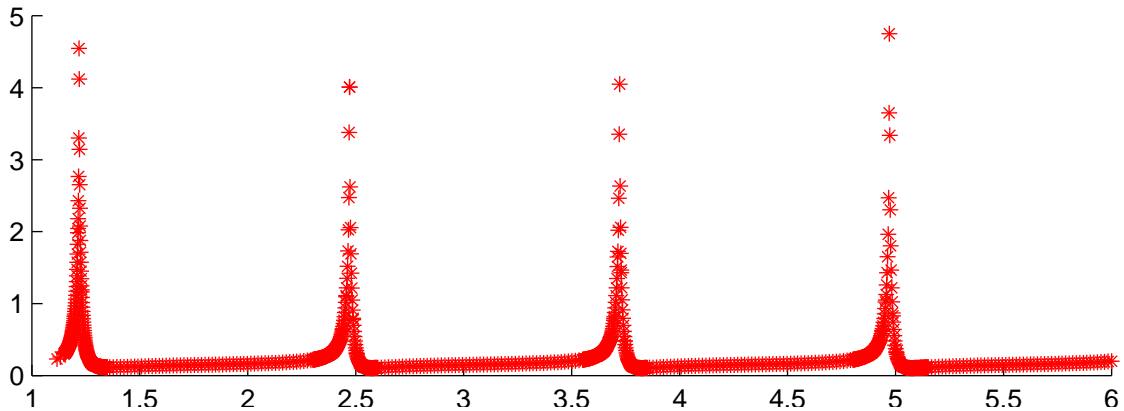


Figure 5: Curve $L \mapsto -\ln |s_{12}(L)|$ for $L \in (1.1; 6)$. The peaks correspond to the values of L for which there is zero transmission in ω_L .

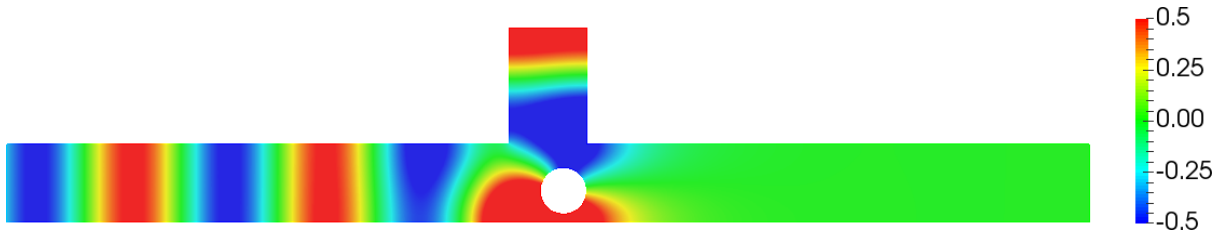


Figure 6: Real part of the total field u_1 defined in (3) for a setting where $s_{12}(L) = 0$ ($L = 2.496$). The incident field is coming from the left.

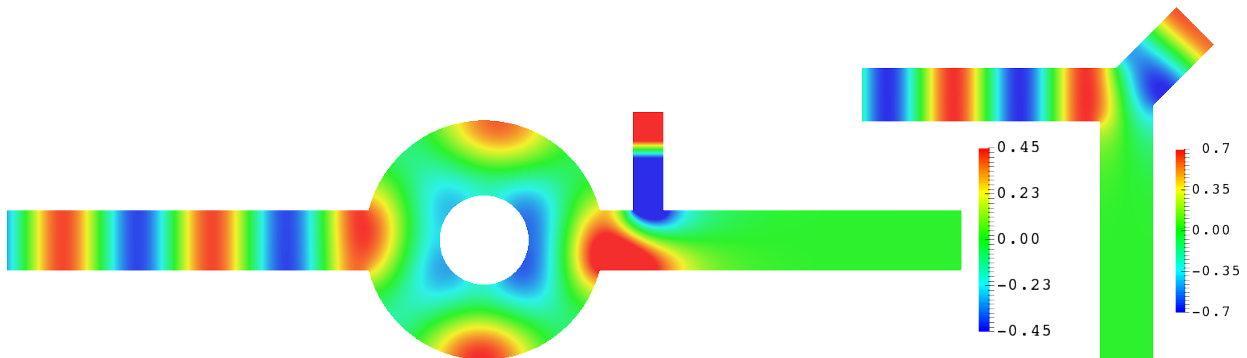


Figure 7: Real part of the total field in two other geometries where the transmission coefficient is zero. For the picture on left, we played with the height of the vertical branch. For the picture on right, we played with the length of the diagonal branch (the waveguide is unbounded in the left and down directions). The incident field is coming from the left.

4.2 Trapped modes

In the second series of experiments, we set $M := (0.2, 0.4)$ as in §4.1, $L := 2.496$ (this is the value obtained in the numerical experiments leading to Figure 6) and, for $\mathcal{L} > 0$,

$$\Omega_{\mathcal{L}} := \{(x, y) \in (-\infty; 1/2 + \mathcal{L}) \times (0; 1) \cup (-1/2; 1/2) \times [1; L]\} \setminus \overline{B(M, 0.3)}.$$

The domain $\Omega_{\mathcal{L}}$ is pictured in Figure 11. According to the results of §4.1, we know that $s_{12} = 0$ in Ω_{∞} (zero transmission) at the wavenumber $k = 0.8\pi$. For each \mathcal{L} in a given range, we compute numerically the coefficients of the augmented scattering matrix $\mathcal{S} \in \mathbb{C}^{2 \times 2}$ defined in (17). To proceed, again we use a P2 finite element method set in a truncated waveguide. We emphasize here that we need to work with a well-suited Dirichlet-to-Neumann map to deal with the wave packet W_2^+ appearing in the decompositions of U_1, U_2 in (16). In Figures 8, 9, 10, we display the coefficients $\mathcal{L} \mapsto S_{11}(\mathcal{L})$, $\mathcal{L} \mapsto S_{12}(\mathcal{L})$, $\mathcal{L} \mapsto S_{22}(\mathcal{L})$ for $\mathcal{L} \in (0.1; 3.5)$ and respectively $k = 0.78\pi$, $k = 0.8\pi$, $k = 0.82\pi$. In these figures, we also display the asymptotic circles Γ_{11}, Γ_{12} and Γ_{22} defined in (20). In accordance with the results of §3.2, we observe that asymptotically as $L \rightarrow +\infty$, the coefficients $\mathcal{L} \mapsto S_{11}(\mathcal{L})$, $\mathcal{L} \mapsto S_{12}(\mathcal{L})$, $\mathcal{L} \mapsto S_{22}(\mathcal{L})$ run respectively on $\Gamma_{11}, \Gamma_{12}, \Gamma_{22}$. Moreover, the curves $\mathcal{L} \mapsto S_{12}(\mathcal{L})$ pass through zero (Proposition 3.1). In Figure 9, we see that for $k = 0.8\pi$, the circle Γ_{22} passes through the point of affix $-1 + 0i$ as shown in Proposition 3.2. Comparing Figures 8, 9 and 10, we observe that the center Z_{22} of Γ_{22} passes from the upper half plane to the lower half plane as k goes from $0.8\pi^-$ to $0.8\pi^+$. As a consequence, we are tempted to think that the map $k \mapsto \Im m Z_{22}(k)$ changes sign at $k = 0.8\pi$ (Assumption (27)). In Figure 11 we display a trapped mode in $\Omega_{\mathcal{L}}$ for $\mathcal{L} = 1.354$ at the wavenumber $k = 2.512... \approx 0.8\pi$. Figure 12 represents the symmetrised version with respect to the line $\{x = H + \mathcal{L}\}$ of the trapped mode of Figure 11.

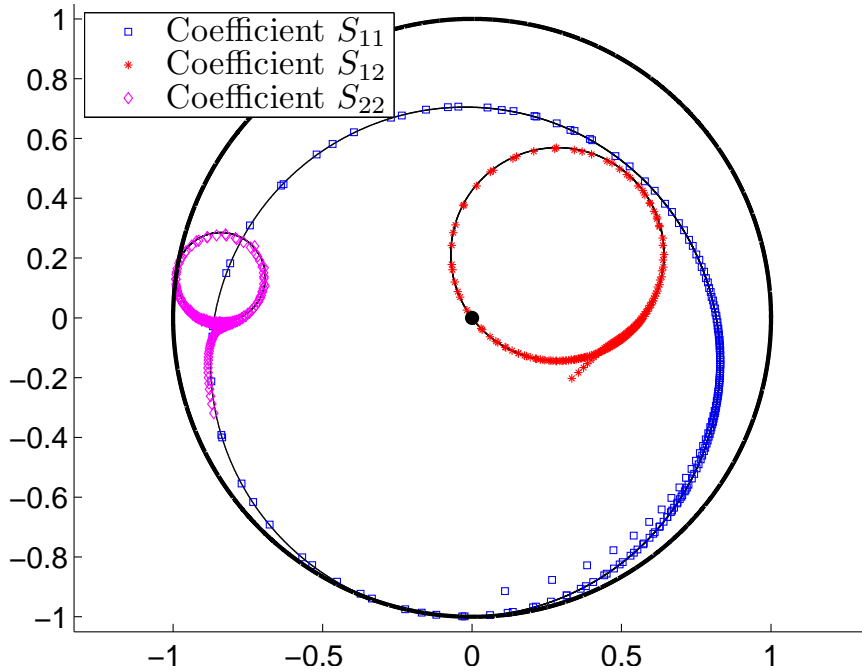


Figure 8: Coefficients $\mathcal{L} \mapsto S_{11}(\mathcal{L})$, $\mathcal{L} \mapsto S_{12}(\mathcal{L})$ and $\mathcal{L} \mapsto S_{22}(\mathcal{L})$ for $\mathcal{L} \in (0.1; 3.5)$. The thin black circles (mostly hidden by the symbols) correspond to the asymptotic circles Γ_{11} , Γ_{12} and Γ_{22} defined in (20). Here $k = 0.78\pi$.

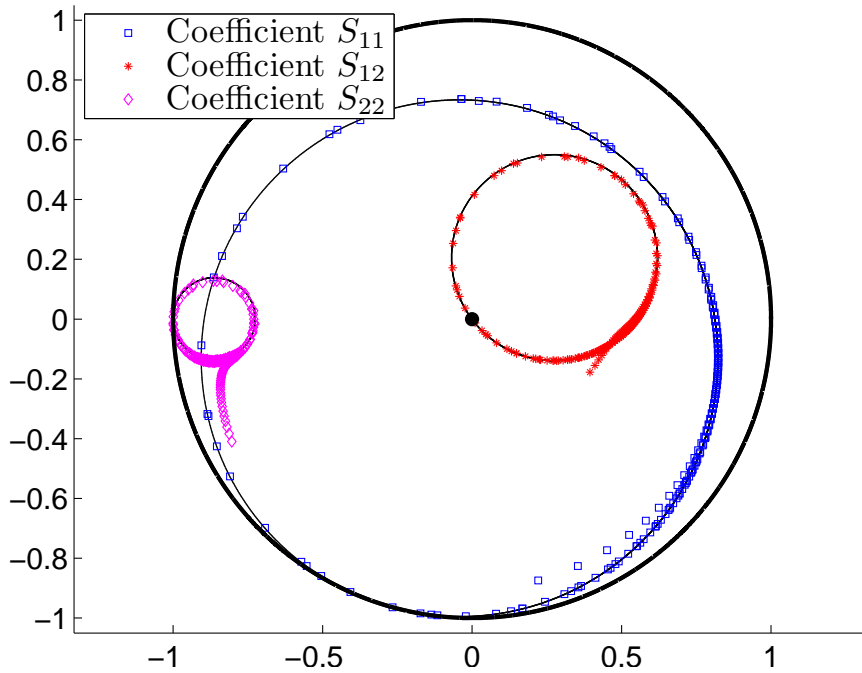


Figure 9: Coefficients $\mathcal{L} \mapsto S_{11}(\mathcal{L})$, $\mathcal{L} \mapsto S_{12}(\mathcal{L})$ and $\mathcal{L} \mapsto S_{22}(\mathcal{L})$ for $\mathcal{L} \in (0.1; 3.5)$. The thin black circles (mostly hidden by the symbols) correspond to the asymptotic circles Γ_{11} , Γ_{12} and Γ_{22} defined in (20). Here $k = 0.8\pi$.

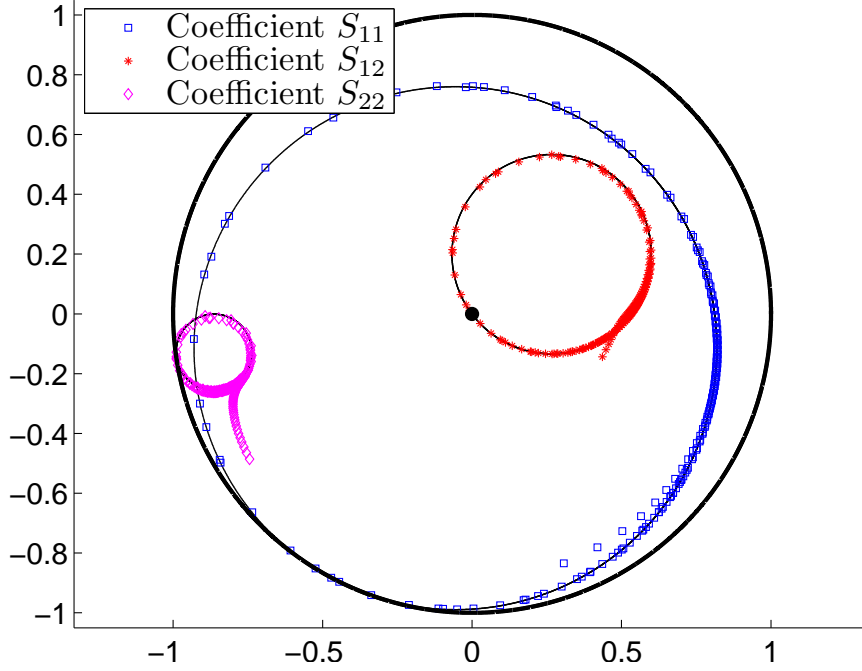


Figure 10: Coefficients $\mathcal{L} \mapsto S_{11}(\mathcal{L})$, $\mathcal{L} \mapsto S_{12}(\mathcal{L})$ and $\mathcal{L} \mapsto S_{22}(\mathcal{L})$ for $\mathcal{L} \in (0.1; 3.5)$. The thin black circles (mostly hidden by the symbols) correspond to the asymptotic circles Γ_{11} , Γ_{12} and Γ_{22} defined in (20). Here $k = 0.82\pi$.

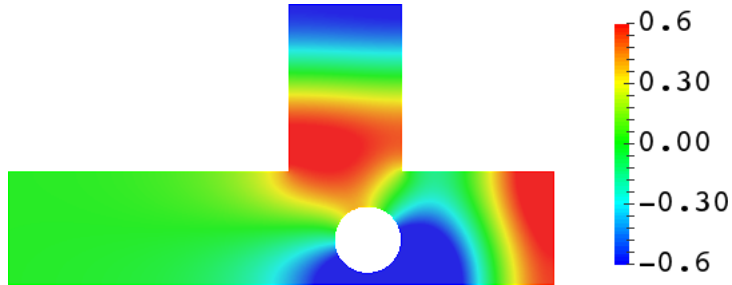


Figure 11: Trapped mode for Problem (2) in $\Omega_{\mathcal{L}}$. Here $k = 2.5125645 \approx 0.8\pi$ and $\mathcal{L} = 1.354$.

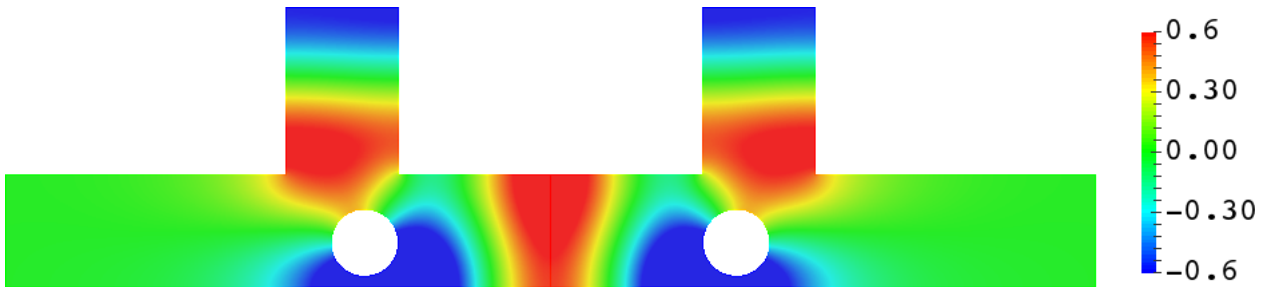


Figure 12: Symmetrization of the trapped mode of Figure 11.

5 Conclusion

In this article, first we explained how to construct waveguides with two open channels such that the transmission coefficient in monomode regime is zero. In that case, the energy carried by an ingoing mode propagating in one channel is completely backscattered, this is the mirror effect. The principal novelty of this study is that there is no assumption of symmetry of the geometry. Then in a second step, from a geometry where it is known that the transmission coefficient is zero, truncating one of the channel, we showed how to create half-waveguides supporting trapped modes. All the techniques presented here can be adapted in higher dimension (waveguides of \mathbb{R}^d with $d \geq 3$). Moreover, Neumann boundary conditions can be replaced by Dirichlet boundary conditions, the developments are exactly the same. For the construction of completely reflecting geometries, we have assumed that outside a compact domain, the waveguide coincides with the strip $\mathbb{R} \times (0; 1)$. This is not needed in the analysis and configurations like the ones of Figure 7 right or Figure 13 top can be considered as well. More precisely, the two open channels can be oriented in different directions and their height can differ. Similarly, to provide examples of half-waveguides supporting trapped modes, we can start from geometries as the ones of Figure 13 top such that the transmission coefficient is zero and truncate one branch.

To continue this work, there are many directions to investigate. Dealing with the case of waveguides with N open channels for $N \geq 3$ (see Figure 13 bottom) seems an interesting one. For this problem, again several questions can be considered. For example, can one find a geometry such that the energy carried by an ingoing mode propagating in one channel is completely backscattered? In this case, we have to cancel $N - 1$ transmission coefficients (s_{12}, \dots, s_{1N}). Playing with one branch is probably not enough. Can we do it with $N - 1$ branches? And then, starting from a geometry like the one of Figure 13 bottom where the mirror effect occurs ($s_{12} = \dots = s_{1N} = 0$), truncating channel 1, can we create waveguides supporting trapped modes? This sounds more easily achievable. Another interesting direction would be to study what happens at higher wavenumber when several modes can propagate. For the moment, this is highly open.

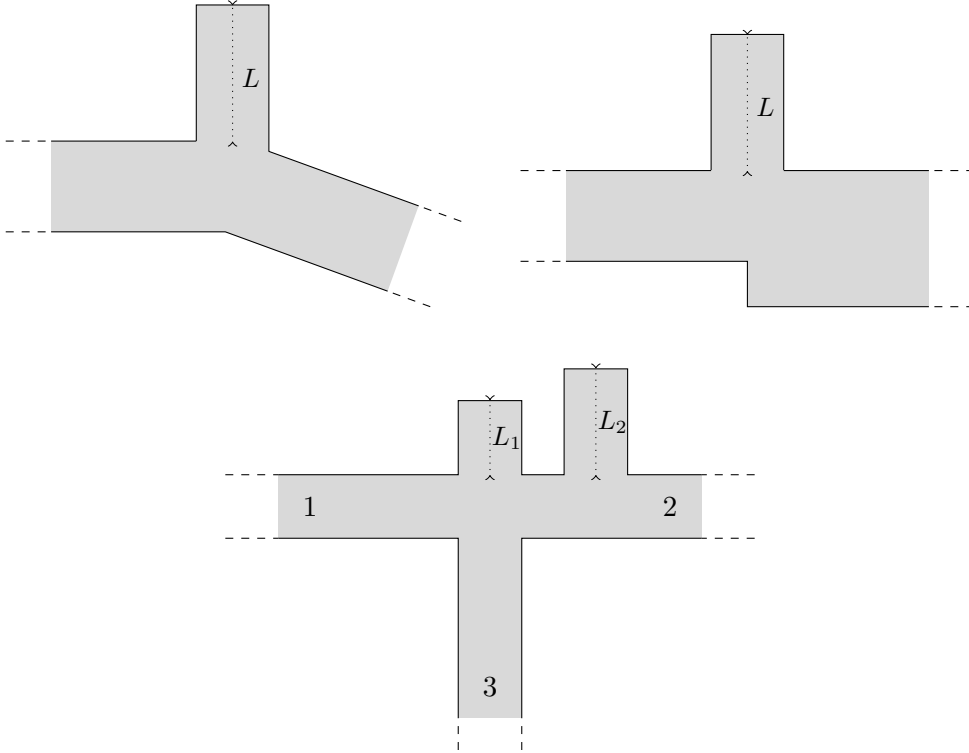


Figure 13: Top: other types of waveguides where the approaches presented above work. Bottom: example of waveguide with three open channels.

In Figure 14, we represent another geometry ω_L where the branch of finite length used in the article has been replaced by a half disk of radius L . We also add a fixed non penetrable (Neumann) obstacle in the domain to break the symmetry of the geometry. In Figure 15 left, we computed the scattering coefficients (see (3)) with respect to $L \in (0.5; 2)$. Again we observe that even though ω_L is completely not symmetric, the transmission coefficient passes through zero as L increases. This is confirmed when we draw the curve $L \mapsto -\ln |s_{12}(L)|$ (Figure 15 top right). In Figure 15 bottom right, we represent the real part of the total field in a situation where the transmission coefficient is zero. All that results are numerical results. It would be interesting to prove them rigorously. However the asymptotic analysis for this problem is different from the one presented above.

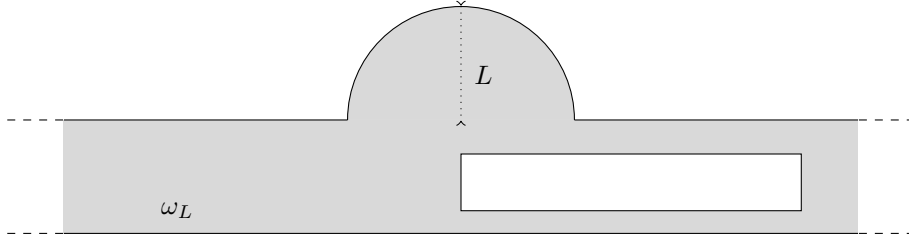


Figure 14: Geometry of ω_L .

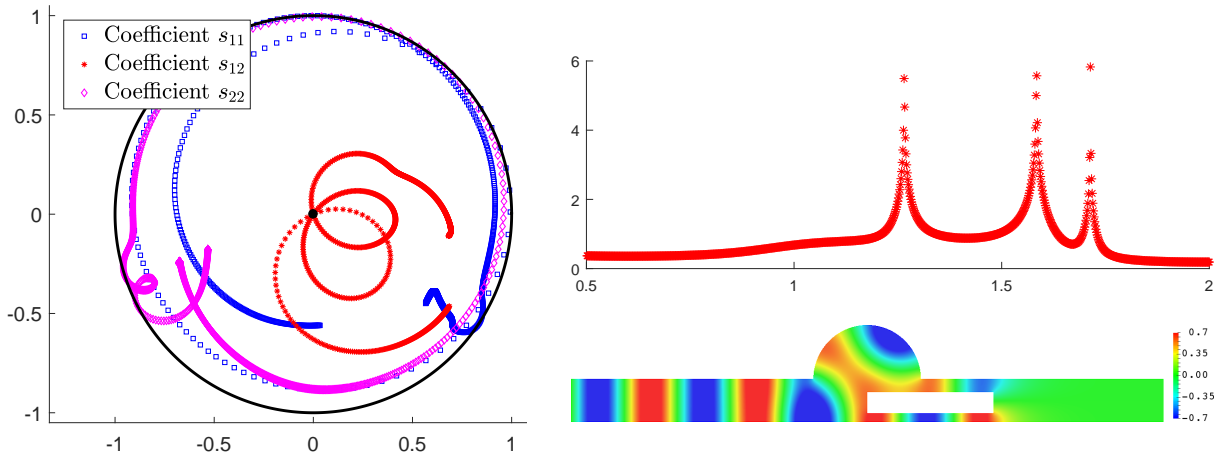


Figure 15: Left: coefficients $L \mapsto s_{11}(L)$, $L \mapsto s_{12}(L)$ and $L \mapsto s_{22}(L)$ for $L \in (0.5; 2)$ in the geometry of Figure 14. According to the conservation of energy, we know that the scattering coefficients are located inside the unit disk marked by the black bold line. Top right: curve $L \mapsto -\ln |s_{12}(L)|$ for $L \in (0.5; 2)$. Bottom right: real part of the total field u_1 defined in (3) for a setting where $s_{12}(L) = 0$ ($L = 1.265488$). The incident field is coming from the left.

6 Annex

6.1 Properties of the scattering matrices

In this paragraph, for the convenience of the reader, we provide the details of the proofs of two results used in the previous analysis. We start with a well-known lemma.

Lemma 6.1. *The scattering matrix \mathbb{S} defined in (4) is unitary and symmetric.*

Proof. Let us work with the symplectic form $q(\cdot, \cdot)$ introduced in (23) such that

$$q(u, v) = \int_{\Sigma_{-2H} \cup \Sigma_{2H}} \frac{\partial u}{\partial n} \bar{v} - u \frac{\partial \bar{v}}{\partial n} d\sigma, \quad \forall u, v \in \mathbb{H}_{\text{loc}}^1(\Omega_L).$$

Integrating by parts and using that the functions u_1, u_2 defined in (3) satisfy the Helmholtz equation, we obtain $q(u_i, u_j) = 0$ for $i, j \in \{1, 2\}$. On the other hand, decomposing u_1, u_2 in Fourier series on $\Sigma_{\pm 2H}$, we find

$$\begin{aligned} q(u_1, u_1) &= (-1 + |s_{11}|^2 + |s_{12}|^2) i, & q(u_2, u_2) &= (-1 + |s_{22}|^2 + |s_{21}|^2) i \\ q(u_1, u_2) &= -\overline{q(u_2, u_1)} = s_{11} \overline{s_{21}} + s_{12} \overline{s_{22}}. \end{aligned}$$

These relations allow us to prove that $\mathbb{S} \overline{\mathbb{S}}^\top = \text{Id}^{2 \times 2}$, that is to conclude that \mathbb{S} is unitary. On the other hand, one finds $q(u_1, \overline{u_2}) = 0 = -s_{21} + s_{12}$. We deduce that \mathbb{S} is symmetric. \square

Lemma 6.2. *For all $L > 1$, the matrix $\mathbb{S}^{\text{asy}}(L) \in \mathbb{C}^{2 \times 2}$ defined in (8) is unitary.*

Proof. A direct computation using the definitions of the coefficients of $\mathbb{S}^{\text{asy}}(L)$ (see (9)) gives

$$\begin{aligned} |s_{11}^{\text{asy}}|^2 + |s_{12}^{\text{asy}}|^2 &= |s_{11}^\infty|^2 + |s_{12}^\infty|^2 + \frac{|s_{13}^\infty|^2 (|s_{13}^\infty|^2 + |s_{23}^\infty|^2)}{|e^{-2ikL} - s_{33}^\infty|^2} + 2\Re e \frac{s_{13}^\infty (\overline{s_{11}^\infty} s_{13}^\infty + \overline{s_{12}^\infty} s_{23}^\infty)}{e^{-2ikL} - s_{33}^\infty} \\ &= |s_{11}^\infty|^2 + |s_{12}^\infty|^2 + \frac{|s_{13}^\infty|^2 (1 - |s_{33}^\infty|^2)}{|e^{-2ikL} - s_{33}^\infty|^2} - 2|s_{13}^\infty|^2 \Re e \frac{\overline{s_{33}^\infty}}{e^{-2ikL} - s_{33}^\infty} \\ &= |s_{11}^\infty|^2 + |s_{12}^\infty|^2 + |s_{13}^\infty|^2 \frac{|e^{-2ikL} - s_{33}^\infty|^2}{|e^{-2ikL} - s_{33}^\infty|^2} = 1. \end{aligned}$$

To obtain the equalities above, we used several times the fact that $\mathbb{S}^\infty \in \mathbb{C}^{3 \times 3}$ is unitary. Analogously, one finds $|s_{12}^{\text{asy}}|^2 + |s_{22}^{\text{asy}}|^2 = 1$. On the other hand, we have

$$\begin{aligned} &s_{11}^{\text{asy}} \overline{s_{12}^{\text{asy}}} + s_{12}^{\text{asy}} \overline{s_{22}^{\text{asy}}} \\ &= s_{11}^\infty \overline{s_{12}^\infty} + s_{12}^\infty \overline{s_{22}^\infty} + \frac{|s_{13}^\infty|^2 s_{13}^\infty \overline{s_{23}^\infty} + |s_{23}^\infty|^2 s_{13}^\infty \overline{s_{23}^\infty}}{|e^{-2ikL} - s_{33}^\infty|^2} + \frac{s_{13}^\infty (s_{13}^\infty \overline{s_{12}^\infty} + s_{23}^\infty \overline{s_{22}^\infty})}{e^{-2ikL} - s_{33}^\infty} + \frac{\overline{s_{23}^\infty} (s_{11}^\infty \overline{s_{13}^\infty} + s_{12}^\infty \overline{s_{23}^\infty})}{e^{2ikL} - \overline{s_{33}^\infty}} \\ &= s_{11}^\infty \overline{s_{12}^\infty} + s_{12}^\infty \overline{s_{22}^\infty} + s_{13}^\infty \overline{s_{23}^\infty} \frac{1 - |s_{33}^\infty|^2}{|e^{-2ikL} - s_{33}^\infty|^2} - \frac{s_{13}^\infty s_{33}^\infty \overline{s_{23}^\infty}}{e^{-2ikL} - s_{33}^\infty} - \frac{\overline{s_{23}^\infty} s_{13}^\infty \overline{s_{33}^\infty}}{e^{2ikL} - \overline{s_{33}^\infty}} \\ &= s_{11}^\infty \overline{s_{12}^\infty} + s_{12}^\infty \overline{s_{22}^\infty} + s_{13}^\infty \overline{s_{23}^\infty} = 0. \end{aligned}$$

Since $\mathbb{S}^{\text{asy}}(L)$ is symmetric, this is sufficient to conclude that $\mathbb{S}^{\text{asy}}(L)$ is unitary. \square

6.2 Particular cases in the asymptotic analysis of the scattering matrices

When $|s_{33}^\infty| = 1$, the asymptotic (9) of the scattering matrix \mathbb{S} with respect to L is different from what has been obtained above. More precisely, if $|s_{33}^\infty| = 1$, since \mathbb{S}^∞ is unitary and symmetric, then $s_{31}^\infty = s_{32}^\infty = 0$, $s_{13}^\infty = s_{23}^\infty = 0$. In such a situation, we can show that as $L \rightarrow +\infty$, the matrix $\mathbb{S} = \mathbb{S}(L)$ defined in (4) tends to

$$\begin{pmatrix} s_{11}^\infty & s_{12}^\infty \\ s_{21}^\infty & s_{22}^\infty \end{pmatrix} \in \mathbb{C}^{2 \times 2}.$$

A similar phenomenon appears in the asymptotic (19) of \mathcal{S} when $|S_{33}^\infty| = 1$. In this situation, we have $S_{31}^\infty = S_{32}^\infty = 0$, $S_{13}^\infty = S_{23}^\infty = 0$ and one can prove that \mathcal{S} tends to

$$\begin{pmatrix} S_{11}^\infty & S_{12}^\infty \\ S_{21}^\infty & S_{22}^\infty \end{pmatrix} \in \mathbb{C}^{2 \times 2}.$$

In this article, we do not consider these exceptional cases which are not interesting for our analysis.

References

- [1] G.S. Abeynanda and S.P. Shipman. Dynamic resonance in the high-Q and near-monochromatic regime. *MMET, IEEE*, 10.1109/MMET.2016.7544100, 2016.
- [2] A. Aslanyan, L. Parnovski, and D. Vassiliev. Complex resonances in acoustic waveguides. *Quart. J. Mech. Appl. Math.*, 53(3):429–447, 2000.
- [3] E. Bulgakov and A. Sadreev. Formation of bound states in the continuum for a quantum dot with variable width. *Phys. Rev. B*, 83(23):235321, 2011.
- [4] G. Cattapan and P. Lotti. Bound states in the continuum in two-dimensional serial structures. *Eur. Phys. J. B*, 66(4):517–523, 2008.
- [5] L. Chesnel and S.A. Nazarov. Non reflection and perfect reflection via Fano resonance in waveguides. *Commun. Math. Sci.*, to appear, *arXiv preprint arXiv:1801.08889*, 2018.
- [6] L. Chesnel, S.A. Nazarov, and V. Pagneux. Invisibility and perfect reflectivity in waveguides with finite length branches. *SIAM J. Appl. Math.*, 78(4):2176–2199, 2018.
- [7] L. Chesnel and V. Pagneux. Simple examples of perfectly invisible and trapped modes in waveguides. *Quart. J. Mech. Appl. Math.*, 71(3):297–315, 2018.
- [8] E.B. Davies and L. Parnovski. Trapped modes in acoustic waveguides. *Q. J. Mech. Appl. Math.*, 51(3):477–492, 1998.
- [9] Y. Duan, W. Koch, C.M. Linton, and M. McIver. Complex resonances and trapped modes in ducted domains. *J. Fluid. Mech.*, 571:119–147, 2007.
- [10] D.V. Evans. Trapped acoustic modes. *IMA J. Appl. Math.*, 49(1):45–60, 1992.
- [11] D.V. Evans, M. Levitin, and D. Vassiliev. Existence theorems for trapped modes. *J. Fluid. Mech.*, 261:21–31, 1994.
- [12] D.V. Evans and C.M. Linton. Trapped modes in open channels. *J. Fluid. Mech.*, 225:153–175, 1991.
- [13] U. Fano. Effects of configuration interaction on intensities and phase shifts. *Phys. Rev.*, 124(6):1866–1878, 1961.
- [14] H. Friedrich and D. Wintgen. Interfering resonances and bound states in the continuum. *Phys. Rev. A*, 32(6):3231, 1985.
- [15] J. Gomis-Bresco, D. Artigas, and L. Torner. Anisotropy-induced photonic bound states in the continuum. *Nat. Photon.*, 11(4):232, 2017.
- [16] J.W. González, M. Pacheco, L. Rosales, and P.A. Orellana. Bound states in the continuum in graphene quantum dot structures. *Europhys. Lett.*, 91(6):66001, 2010.
- [17] S. Hein, W. Koch, and L. Nannen. Trapped modes and Fano resonances in two-dimensional acoustical duct–cavity systems. *J. Fluid. Mech.*, 692:257–287, 2012.
- [18] P. Henrici. *Applied and computational complex analysis*. Wiley-Interscience, 1974. Volume 1: Power series—integration—conformal mapping—location of zeros, Pure and Applied Mathematics.
- [19] C.W. Hsu, B. Zhen, A.D. Stone, J.D. Joannopoulos, and M. Soljačić. Bound states in the continuum. *Nat. Rev. Mater.*, 1:16048, 2016.
- [20] I.V. Kamotskiĭ and S.A. Nazarov. An augmented scattering matrix and exponentially decreasing solutions of an elliptic problem in a cylindrical domain. *Zap. Nauchn. Sem. S.-Peterburg. Otdel. Mat. Inst. Steklov. (POMI)*, 264(Mat. Vopr. Teor. Rasprostr. Voln. 29):66–82, 2000. (English transl.: *J. Math. Sci.* 2002. V. 111, N 4. P. 3657–3666).
- [21] N. Kuznetsov and P. McIver. On uniqueness and trapped modes in the water-wave problem for a surface-piercing axisymmetric body. *Q. J. Mech. Appl. Math.*, 50(4), 1997.
- [22] C.M. Linton and P. McIver. Embedded trapped modes in water waves and acoustics. *Wave motion*, 45(1):16–29, 2007.
- [23] V.G. Maz’ya, S.A. Nazarov, and B.A. Plamenevskiĭ. *Asymptotic theory of elliptic boundary value problems in singularly perturbed domains, Vol. 1*. Birkhäuser, Basel, 2000. Translated from the original German 1991 edition.
- [24] M. McIver. An example of non-uniqueness in the two-dimensional linear water wave problem. *J. Fluid. Mech.*, 315:257–266, 1996.

- [25] A.E. Miroshnichenko, S. Flach, and Y.S. Kivshar. Fano resonances in nanoscale structures. *Rev. Mod. Phys.*, 82(3):2257–2298, 2010.
- [26] N. Moiseyev. Suppression of Feshbach resonance widths in two-dimensional waveguides and quantum dots: a lower bound for the number of bound states in the continuum. *Phys. Rev. Lett.*, 102(16):167404, 2009.
- [27] S.A. Nazarov. A criterion for the existence of decaying solutions in the problem on a resonator with a cylindrical waveguide. *Funct. Anal. Appl.*, 40(2):97–107, 2006.
- [28] S.A. Nazarov. Sufficient conditions on the existence of trapped modes in problems of the linear theory of surface waves. *J. Math. Sci.*, 167(5):713–725, 2010.
- [29] S.A. Nazarov. Trapped modes in a T-shaped waveguide. *Acoust. Phys.*, 56(6):1004–1015, 2010.
- [30] S.A. Nazarov. Asymptotic expansions of eigenvalues in the continuous spectrum of a regularly perturbed quantum waveguide. *Theor. Math. Phys.*, 167(2):606–627, 2011.
- [31] S.A. Nazarov. Enforced stability of a simple eigenvalue in the continuous spectrum of a waveguide. *Funct. Anal. Appl.*, 47(3):195–209, 2013.
- [32] S.A. Nazarov and B.A. Plamenevskiĭ. *Elliptic problems in domains with piecewise smooth boundaries*, volume 13 of *Expositions in Mathematics*. De Gruyter, Berlin, Germany, 1994.
- [33] S.A. Nazarov and B.A. Plamenevskiĭ. Selfadjoint elliptic problems: scattering and polarization operators on the edges of the boundary. *Algebra i Analiz*, 6(4):157–186, 1994. (English transl.: *Sb. Math. J.* 1995. V. 6, N 4. P. 839–863).
- [34] S.A. Nazarov and A.V. Shanin. Calculation of characteristics of trapped modes in t-shaped waveguides. *Computational Mathematics and Mathematical Physics*, 51(1):96–110, 2011.
- [35] J. Okołowicz, M. Płoszajczak, and I. Rotter. Dynamics of quantum systems embedded in a continuum. *Phys. Rep.*, 374(4):271–383, 2003.
- [36] G. Ordóñez, K. Na, and S. Kim. Bound states in the continuum in quantum-dot pairs. *Phys. Rev. A*, 73(2):022113, 2006.
- [37] V. Pagneux. Trapped modes and edge resonances in acoustics and elasticity. In *Dynamic Localization Phenomena in Elasticity, Acoustics and Electromagnetism*, pages 181–223. Springer, 2013.
- [38] R. Parker. Resonance effects in wake shedding from parallel plates: some experimental observations. *J. Sound Vib.*, 4(1):62–72, 1966.
- [39] R. Parker. Resonance effects in wake shedding from parallel plates: Calculation of resonant frequencies. *J. Sound Vib.*, 5(2):330–343, 1967.
- [40] R. Porter. Trapping of water waves by pairs of submerged cylinders. *Proc. R. Soc. A*, 458(2019):607–624, 2002.
- [41] A.F. Sadreev, E.N. Bulgakov, and I. Rotter. Bound states in the continuum in open quantum billiards with a variable shape. *Phys. Rev. B*, 73(23):235342, 2006.
- [42] Y. Sato, Y. Tanaka, J. Upham, Y. Takahashi, T. Asano, and S. Noda. Strong coupling between distant photonic nanocavities and its dynamic control. *Nat. Photon.*, 6(1):56–61, 2012.
- [43] S.P. Shipman and H. Tu. Total resonant transmission and reflection by periodic structures. *SIAM J. Appl. Math.*, 72(1):216–239, 2012.
- [44] S.P. Shipman and S. Venakides. Resonant transmission near nonrobust periodic slab modes. *Phys. Rev. E*, 71(2):026611, 2005.
- [45] S.P. Shipman and A.T. Welters. Resonant electromagnetic scattering in anisotropic layered media. *J. Math. Phys.*, 54(10):103511, 2013.
- [46] F. Ursell. Trapping modes in the theory of surface waves. *Proc. Camb. Philos. Soc.*, 47:347–358, 1951.
- [47] B. Zhen, C.W. Hsu, L. Lu, A.D. Stone, and M. Soljačić. Topological nature of optical bound states in the continuum. *Phys. Rev. Lett.*, 113(25):257401, 2014.